THE ASTROPHYSICAL JOURNAL, 449:839–862, 1995 August 20

CNO ABUNDANCES AND THE EVOLUTIONARY STATUS OF GALACTIC, A-TYPE SUPERGIANTS

KIM A. VENN[1]
Department of Astronomy, University of Texas at Austin; and Max-Planck-Institut für Astrophysik
Received 1994 December 2; accepted 1995 February 13

ABSTRACT

The carbon, nitrogen, and oxygen abundances of 22 massive, Galactic, A-type supergiants are presented in order to study the evolutionary status of these stars. Various evolution scenarios describe vastly different histories for these stars, which can be distinguished by the atmospheric abundances of CNO that they predict. Chemical abundances are determined from observations of weak optical spectral lines gathered at the McDonald Observatory. An atmospheric analysis is performed for each star adopting the most recent Kurucz LTE model atmospheres. Atmospheric parameters and LTE metal abundances for these stars have been presented in Venn (1995).

Non-LTE (NLTE) line formation calculations have been carried out for the nitrogen and carbon abundances. For carbon, we adopt the Stürenburg & Holweger (1990) model atom and extensively test the effects of the atomic data on the resultant NLTE corrections. We find significant NLTE corrections [$=\log \epsilon(\mathrm{X})_{\mathrm{NLTE}} - \log \epsilon(\mathrm{X})_{\mathrm{LTE}}$] for the cooler supergiants that range from -0.1 in the F0 stars to -0.5 in the A3 stars. The mean NLTE carbon abundance is $\log \epsilon(\mathrm{C})_{\mathrm{NLTE}} = 8.14 \pm 0.13$ for the 14 A3–F0 supergiants. For the hotter stars, we show that the only C I lines that we have observed near 9100 Å do not yield reliable elemental abundances. For nitrogen, we have constructed a new, detailed model atom (Lemke & Venn 1995). Application of this model atom to the A-type supergiants shows that departures from LTE strongly affect the nitrogen abundances. NLTE corrections for weak lines are quite large, ranging from -1.0 dex in the A0 supergiants to -0.3 in the F0 supergiants. The average NLTE nitrogen abundance is $\log \epsilon(\mathrm{N})_{\mathrm{NLTE}} = 8.05 \pm 0.19$ for the 22 A0–F0 supergiants. These NLTE abundances do not show the strong dependence on the effective temperature that we observed in the LTE nitrogen abundances.

When the NLTE nitrogen and carbon abundances of the A3–F0 supergiants are compared to those of the main-sequence B stars, we find $[\log \epsilon(\mathrm{N/C})_{\mathrm{AI}} - \log \epsilon(\mathrm{N/C})_{\mathrm{B*}}] = +0.38 \pm 0.26$. This value is significantly less than the first dredge-up abundances ($\sim +0.65$ for 10 $M_\odot$ stars) predicted by several evolution scenarios. However, the nonzero [N/C] ratio suggests that the A-type supergiants have undergone some *partial* mixing of CN-cycled gas. This is similar to recent abundance results for some B-type supergiants (Gies & Lambert 1992; Lennon 1994), suggesting that partial mixing may occur near the main-sequence (possibly by turbulent diffusive mixing; Maeder 1987; Denissenkov 1994). We conclude that the 5–20 $M_\odot$ A-type supergiants in the Galaxy have evolved directly from the main sequence.

Subject headings: radiative transfer — stars: abundances — stars: atmospheres — stars: early-type — stars: evolution — supergiants

1. INTRODUCTION

To understand the chemical evolution of our Galaxy, we must have a clear picture of the evolution of its massive stars. These stars are important sites for the nucleosynthesis of the chemical elements, which are returned to the interstellar medium through supernovae events and stellar winds. One group of massive stars in the Galaxy that represent an unexplored piece of the chemical abundance puzzle are the A-type supergiants located in the Galactic disk. These stars, with masses between 5 and 20 solar masses, are only moderately evolved, which puts them in a propitious phase for a study of the evolution of massive stars. Specifically, various evolutionary scenarios predict vastly different histories for these stars, which should be distinguishable by the CNO contents in the A supergiant atmospheres. The chemical abundances in A supergiants have been relatively unexplored in the past, but there are good reasons for this inattention. There are no suggestions from their spectra that there is anything odd in their chemical compositions, and their stellar atmospheres are very difficult to model effectively for reliable abundance determinations. Modern techniques alleviate some of these model atmosphere problems, such that we have pursued a detailed abundance analysis of a sample of A-type supergiants in order to help constrain the evolutionary scenarios for massive stars.

1.1. *The Uncertain Evolutionary Status of A-Type Supergiants*

Different evolutionary scenarios for massive (5–20 $M_\odot$) stars can be derived depending on the initial physical assumptions made for the evolution calculations, in particular, for the convection criterion, mass-loss rates, metallicity, and treatment of convective overshooting. These are reviewed by Langer & Maeder (1995) and Fitzpatrick & Garmany (1990) and are discussed briefly here.

Many stellar evolution calculations at solar metallicities (El Eid 1994; Langer 1994; Bressan et al. 1993; Schaller et al. 1992; Stothers & Chin 1991 for $M \geq 10\ M_\odot$; Maeder & Meynet 1989; Chiosi, Nasi, & Sreenivasan 1978; Stothers & Chin 1973, and references therein) predict that the inter-

[1] Current address: Institut für Astronomie und Astrophysik, Scheinerstrasse 1, 81679, München, Germany.

mediate-mass, A supergiants are in a phase of helium core burning. Core helium ignition occurs when the star is a blue supergiant, but thermal instabilities cause the star to immediately expand to the red supergiant region. As a red supergiant, the star is able to resume thermal and radiative equilibrium through convection in the outer layers, and it returns to the A-type supergiant region for most of its He-core burning lifetime. If a massive star evolves quickly off the main sequence to the red giant branch (RGB), then the development of a deep surface convection zone mixes gas from the hydrogen-burned layers into the observable stellar envelope (first dredge-up). Hydrogen burning on the main sequence primarily occurs via the CNO cycle in massive stars. Thus, the first dredge-up causes the surface abundances of carbon, nitrogen, and oxygen to be altered in a discernible way (C decreases by $\sim$0.15 dex, N is enriched by $\sim$0.5 dex, and O is only slightly reduced by $\sim$0.05 dex), with the sum of the nuclei remaining constant since they only act as catalysts in the cycle. Therefore, in this evolutionary scenario, most A-type supergiants should show first dredge-up CNO abundances. Note that the star would have existed once previously as an A-type supergiant, but thermal instabilities would make the star's first pass through this phase very rapid; e.g., only 1 in 100 ($\pm$50) stars would be in this rapid envelope expansion phase compared to the quiescent, post-RGB helium-burning phase according to the Schaller et al. (1992) calculations.

An alternative scenario is that the A-type supergiants initiate helium core burning without visiting the RGB; hence, they would evolve directly from the main sequence (Stothers & Chin 1991 for $M < 10\ M_{\odot}$; Stothers & Chin 1976, and references therein; Chiosi & Summa 1970; Iben 1966). In this scenario, a fully convective intermediate zone is predicted, such that after He ignition, the envelope is able to establish thermal equilibrium without rapid expansion. Therefore, the star is stable as an A-type supergiant when core He burning begins, and in this case, no mixing with deeper layers is anticipated, hence the CNO abundances should be normal (e.g., like those of main-sequence B stars).

The interesting point is that these evolution scenarios can predict completely different abundances for the CNO elements. If these stars are post-RGB stars, then CNO will resemble the first dredge-up abundance pattern (above), and if these stars have evolved directly from the main sequence, then CNO should resemble normal main-sequence B star abundances. A possible complication is that some evolved B stars (Lennon 1994; Gies & Lambert 1992) have shown evidence of some CN-cycled gas in their atmospheres, contrary to the zeroth-order evolution theory where no physical mechanism for mixing CN-cycled gas is included when stars evolve off the main sequence. Maeder (1987) suggested the physical mechanism for mixing on or near the main sequence could be turbulent diffusion induced by rapid rotation on the main sequence, such that "a fraction of normally redwards evolving stars [may] show CNO ratios intermediate between cosmic and [CN-cycle] equilibrium values." Langer (1992) included internal mixing by turbulent diffusion in 20 $M_{\odot}$ models at LMC metallicities for an evolution scenario for the blue supergiant stars, Sk -69° 202, progenitor star to SN 1987A. More recently, Denissenkov (1994) has used partial mixing by turbulent diffusion to explain the slightly altered CNO abundances found by Gies & Lambert (1992) for evolved, 10 $M_{\odot}$ B stars. Thus, we have an additional possibility for the CNO abundances in A-type supergiants; they could show *partial* mixing of CN-cycled material, but still have evolved directly from the main-sequence.

1.2. *Existing Abundance Analyses of A-Type Supergiants*

Very little CNO abundance work has been done on early A-type supergiants because of the difficulties in modeling their atmospheric physical properties. A little more information exists for F0 supergiants. In this project, we will define A-type supergiants as spanning the temperature range from A0 to F0 and the luminosity range from Ia to II.

The only CNO analyses for Population I, early A-type supergiants known to us are for the A0 Ib star η Leo (HD 87737) by Lambert, Hinkle, & Luck (1989), for the B9 Iab star σ Cyg (HD 202850) by Ivanova & Lyubimkov (1990), for the A0 II star ξ^1 Sgr (HD 175687) by Tomkin & Lambert (1994), and the preliminary LTE results for three of the program stars in this paper by Venn (1993). In general, all of these analyses found CNO abundances that resemble the predicted first dredge-up abundances indicating mixing with deeper stellar layers. Interestingly, however, for HD 87737, a solar boron abundance is reported by Boesgaard & Heacox (1978) from a low signal-to-noise *Copernicus* satellite spectrum of the B II line at 1362 Å. If boron is not depleted in the atmosphere of this star, then this implies that there has been little mixing with the deeper, hotter stellar layers which would destroy boron, in contradiction to the CNO abundances conclusion.

CNO abundance analyses for late A-type and F0 supergiants have been performed for the A7 Ib, high Galactic latitude star HD 148743 by Luck, Bond, & Lambert (1990), and the F0 Ib stars Canopus, α Lep (HD 36673), and ι Car by Luck & Lambert (1985, 1981). Again, the CNO abundances in the F0 supergiants (actually throughout the F–K supergiants range) resemble those after the first dredge-up. For HD 148743, the LTE analysis by Luck et al. (1990) found this star is slightly metal poor ([Fe/H] = -0.35),[2] with CNO *each* being overabundant. From this analysis, and that of three other F supergiants, they conclude that the high-latitude supergiants have a unique chemical composition from other Population I supergiants in the disk. (Our analysis of this star disagrees with this conclusion, discussed later.)

In this paper, we present the CNO abundances of 22 Population I, massive ($\sim$5–20 $M_{\odot}$) A0–F0 supergiants. We will calculate the CNO abundances for these stars from line-blanketed, LTE model atmospheres and examine the *corrections* to the carbon and nitrogen abundances when LTE is *not* assumed in the line formation calculations.

2. OBSERVATIONS

The spectroscopic data for this project have been obtained using the facilities at the McDonald Observatory. High signal-to-noise ratio ($\sim$100–150), high-resolution ($\sim$0.07–0.25 Å pixel^{-1}) observations of weak C I, N I, and O I spectral lines were obtained using the coudé spectrographs and CCD cameras at the 2.1 and 2.7 m telescopes. For more information on the observations and data reduction, see Venn (1995).

Representative spectra for the CNO lines are shown in Figure 1. Spectral lines of C I, N I, and O I have been identified using the Moore (1970, 1975, 1976) multiplet tables. Telluric features were removed if necessary by dividing the spectrum by

[2] Throughout this paper, we adopt the usual spectroscopic notation, namely, $[X] = \log_{10}\epsilon(X)_{star} - \log_{10}\epsilon(X)_{\odot}$ for any abundance quantity X, where $\log\epsilon(X) = \log(N_X/N_H) + 12.0$ for absolute number density abundances.

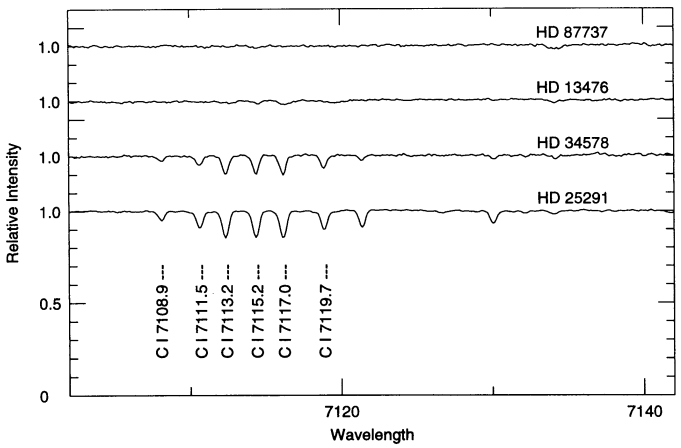

FIG. 1*a*

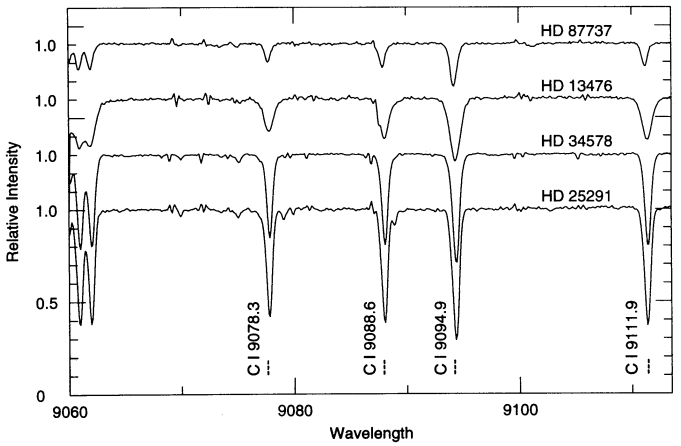

FIG. 1*b*

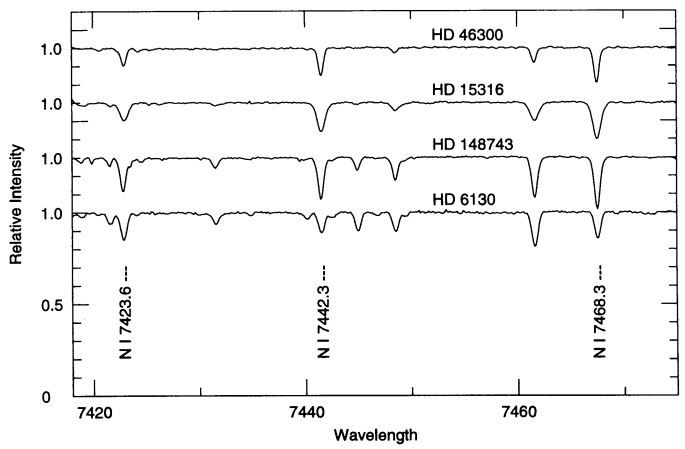

FIG. 1*c*

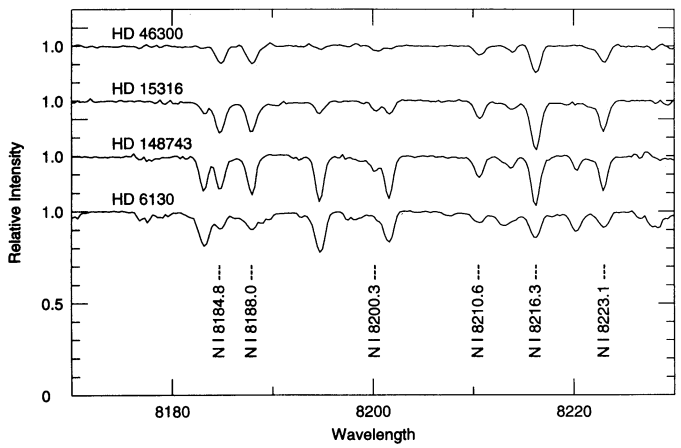

FIG. 1*d*

FIG. 1.—Representative CNO spectra for a variety of stars that span the full range in temperature and gravity of our program. Spectra have been offset for clarity. The following spectral features are shown: (*a*) C I $\lambda\lambda$7115 (telluric features removed), (*b*) C I $\lambda\lambda$9100 (telluric features removed), (*c*) N I $\lambda\lambda$7440, (*d*) N I $\lambda\lambda$8200 (telluric features removed), (*e*) N I $\lambda\lambda$8700 (other N I lines present in the spectrum, but not used in the analysis because they are significantly blended with the Paschen line wing, e.g., three lines near 8685 Å), (*f*) O I $\lambda\lambda$6158, and (*g*) O I $\lambda\lambda$6454 (the telluric features redward of 6457 Å have not been removed and do not necessarily line up in our offset spectra).

that of a rapidly rotating hotter star (O9–B3 stars, with $v \sin i$ greater than 120 km s^{-1}) observed near the same air mass and reduced by the same methods. Most stellar features observed in A stars are not present at much higher temperatures, and the rapid rotation guarantees that any weak lines present will be highly broadened and recognizable. Telluric features were removed from the C I spectra taken near 7115 and 9100 Å, and the N I spectra near 8200 Å. After telluric features were removed, the resultant spectrum often suffered a small degradation in the signal-to-noise ratio due to imperfect cancellations.

3. MODEL ATMOSPHERE ANALYSIS

Chemical abundances have been calculated from a model atmosphere analysis, discussed in detail in Venn (1995). Model atmospheres generated by ATLAS9 (Kurucz 1979, 1991) have been adopted which assume plane-parallel geometry, hydrostatic equilibrium, and LTE. These models are usually sufficient for detailed analyses, although the low surface gravities of A supergiants put them adjacent to the regime where departures from LTE may be significant. A complete analysis of A-type supergiants should also consider effects due to departures from LTE; however, sufficiently line-blanketed NLTE model atmospheres do not currently exist for these stars. Abundances for each program star have been calculated from single spectral lines using the detailed analysis code LINFOR, developed by H. Holweger, W. Steffen, W. Steenbock, and M. Lemke at Kiel University. LINFOR is a standard atmospheric abundances code that can calculate LTE abundances from equivalent width data, or perform spectrum syntheses. First, we checked that the LTE abundances from LINFOR are in agreement with those from WIDTH (since we used this program for the metal line abundances in Venn 1995). When the abundances calculated from LINFOR and WIDTH are compared, we find excellent agreement for most lines of all the elemental species that we examined in these stars, i.e., $\Delta \log \epsilon(\mathrm{X}) \leq 0.02$ (on rare occasions, the difference could be as much as 0.06 dex). The input data for both programs is essentially the same, and we consider the agreement in the abundances between these two independent programs to be very good.

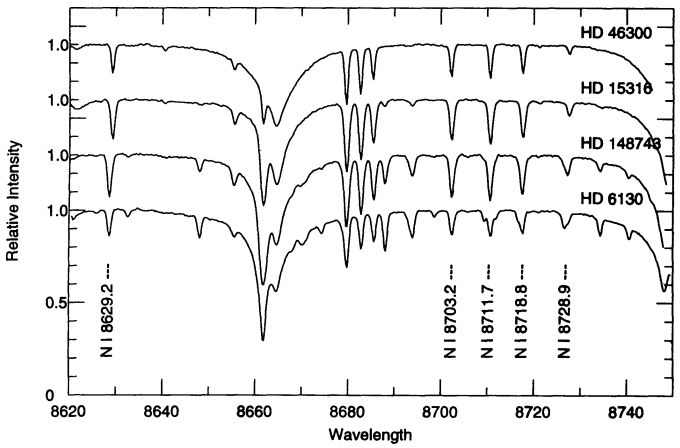

FIG. 1*e*

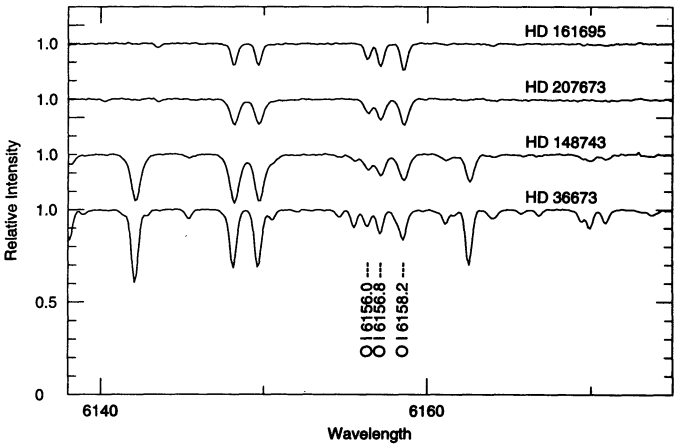

FIG. 1*f*

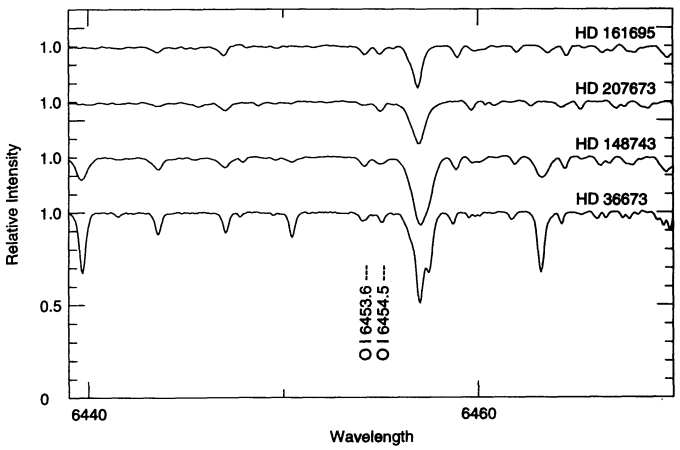

FIG. 1*g*

3.1. *Atomic Data*

Theoretical C I oscillator strengths have been adopted from the Opacity Project (OP) calculations (by Hibbert et al. 1993). These values are in excellent agreement with the values calculated by Nussbaumer & Storey (1984) for multiplet No. 3 near 9100 Å, which Grevesse et al. (1991) discuss as in good agreement with recent radiative lifetime measurements. The theoretical values are also in good agreement with the solar *gf*-values calculated by Lambert, Roby, & Bell (1982) around 7115 Å. Lambert et al. (1982) adopted a solar carbon abundance that is 0.07 dex larger than assumed here; thus, we adjusted the *gf*-values upward by this amount when comparing to the OP values.

N I oscillator strengths have been collected from the experimental radiative lifetime measurements by Zhu et al. (1989). Grevesse et al. (1990) discuss sources for N I oscillator strengths and remark on the excellent agreement between the Zhu et al. values and theoretical predictions by Hibbert et al. (1991a) for the spectral lines observed in this analysis. Zhu et al. estimate the accuracy of their *gf*-values as within 15% (about ± 0.05 dex).

Theoretical *gf*-values have been chosen for the O I spectral lines from OP calculations (by Hibbert et al. 1991b). These results are in excellent agreement with the astrophysically determined values by Lambert et al. (1982) for the λ6158 multiplet lines in the Sun.

3.2. *Atmospheric Parameters*

Atmospheric parameters and the selection of the model atmospheres have been described in detail by Venn (1995). The same model atmosopheres are used in this analysis [where log ϵ(He/H) = 0.1 throughout]. Spectroscopic parameters have been used throughout to determine $T_{\rm eff}$, gravity, and microturbulence values per star; this includes fitting the Hγ line profile and using Mg I/II ionization equilibrium [such that log ϵ(Mg I) = log ϵ(Mg II)] for 19 out of 22 of the program stars. For the other three stars, we did not observe the necessary Mg I lines and used Fe I versus χ (lower excitation potential) as a temperature estimator. The Hγ profiles and Mg ionization equilibrium are sensitive to *both* $T_{\rm eff}$ and gravity, such that a locus of possibilities exists for each spectral parameter in the $T_{\rm eff}$-gravity plane. The intersection point of these two loci was adopted as the atmospheric parameter set for each star. NLTE calculations of the Mg I and Mg II abundances showed that both of these species are very nearly in LTE in the line-forming atmospheric regions. Microturbulence (ξ) was found per star by minimizing the slope in abundance with W_λ for the Fe II, Fe I, and Ti II lines observed. Within our estimated uncertainties, the same ξ-value was found from each elemental species per star.

4. ABUNDANCE RESULTS

All of the line data for the program stars are listed in Table 1. Spectral lines that are significantly blended with other elements have been removed. Lines from crowded spectral regions that are slightly blended with nearby lines have also been excluded if the computed abundances were greater than 2 σ from the mean; this also excludes all lines that occur well into the wings of Balmer lines. Final abundance results are presented in Table 2 as unweighted average abundances per species, along with the line-to-line scatter (σ) and number of lines used in the average. *Only weak lines have been used to compute the averages. Weak lines are defined as those where a change in microturbulence of* ± 1.0 km s^{-1} *yields a change in the derived abundance of less than* 0.1 dex, *with a maximum* $W_\lambda = 200$ mÅ. Strong lines that do not meet this criterion are marked in italics in Table 1 and are *not* included in the final averages (but have been considered when calculating the best values for microturbulence). When fewer than five lines are averaged, σ is probably not a true indictor of the possible error in the abun-

TABLE 1A

SPECTRAL LINE EQUIVALENT WIDTHS

λ	Mult.	χ	Log gf	Ref.	161695	87737	46300	207673	175687	195324	3940	14489	13476	15316	222275
C I:															
4766.62	(6)	7.48	-2.51	op	...	...	...	...	...	...	...	...	...	...	22
4770.00	(6)	7.48	-2.33	op	...	...	...	...	...	...	...	...	...	...	17
4771.72	(6)	7.49	-1.76	op	...	...	...	...	...	...	...	...	...	...	54
4775.87	(6)	7.49	-2.19	op	...	...	...	...	...	...	...	...	...	...	19
7108.94	(25)[a]	8.64	-1.60	op	...	...	...	...	...	...	...	...	...	...	14
7111.48	(26)	8.64	-1.07	op	...	...	...	...	...	...	...	...	...	...	24
7113.18	(26)	8.65	-0.76	op	...	...	...	...	...	...	...	...	12	16	46
7115.19	(26)[b]	8.64	-0.92	op	...	...	...	...	...	...	...	...	10	11	43
7116.99	(25)[a]	8.65	-0.91	op	...	...	...	...	...	...	...	...	17	18	45
7119.67	(25)[a]	8.64	-1.15	op	...	...	...	...	...	...	...	...	10	20	33
9061.48	(3)	7.48	-0.34	op	...	90	80:	120	...	...	...	...	...	...	...
9062.53	(3)	7.48	-0.45	op	...	86	69:	110	...	...	...	...	...	...	...
9078.32	(3)	7.48	-0.58	op	44	58	46	85	56	97	...	28	184	*230*	*248*
9088.57	(3)	7.48	-0.42	op	67	82	63	110	98	119	30:	66	*240*	*239*	*282*
9094.89	(3)	7.49	0.16	op	117	*175*	*145*	*212*	*235*	*253*	80	131	*392*	*430*	*440*
9111.85	(3)	7.49	-0.29	op	70	81	60	93	108	120	30	34	*240*	*291*	*322*
N I:															
6484.88	(21)	11.76	-0.68	op	15	...	...	...	22	20	...	...	...	...	...
7423.63	(3)	10.33	-0.69	zhu	60	74	59	89	95	104	54	102	95	100	115
7442.28	(3)	10.33	-0.40	zhu	97	118	95	*137*	135	*158*	89	*171*	164	153	146
7468.29	(3)	10.34	-0.21	zhu	124	*152*	119	*174*	*157*	*192*	126	*221*	*214*	194	*163*
8184.80	(2)	10.33	-0.29	zhu	...	...	115	*198*	...	*212*	*182*	*278*	*250*	*264*	...
8187.95	(2)	10.33	-0.29	zhu	...	...	120	*198*	...	*240*	*166*	*269*	*251*	*216*	...
8200.31	(2)	10.33	-1.00	zhu	...	...	38	...	...	84	40	...	...	55:	...
8210.64	(2)	10.33	-0.68	zhu	...	...	62	112	...	136	52:	135	128	115	...
8216.28	(2)	10.34	0.09	zhu	...	...	*174*	*303*	...	*305*	*237*	*378*	*358*	*322*	...
8223.07	(2)	10.33	-0.29	zhu	...	...	110	*205*	...	*192*	120	*233*	*218*	193	...
8242.34	(2)	10.34	-0.26	zhu	...	...	107	*207*	...	*192*	137	*226*	*216*	200	...
8629.24	(8)	10.69	0.08	zhu	*133*	*167*	134	*210*	...	*230*	...	...	*269*	*240*	*196*
8703.24	(1)	10.33	-0.34	zhu	*150*	*198*	*156*	*224*	...	*240*	...	...	*279*	*248*	*195*
8711.69	(1)	10.33	-0.24	zhu	*156*	*204*	*161*	*242*	...	*255*	...	...	*306*	*284*	*214*
8718.82	(1)	10.34	-0.35	zhu	*131*	*178*	136	*204*	...	*221*	...	...	*258*	*241*	...
8728.88	(1)	10.33	-1.04	zhu	44	74	47	71	...	96	...	...	91	84:	...
O I:															
6155.99	(10)	10.74	-0.67	op	41	50	41	45	41	53	...	...	42	45	55
6156.78	(10)	10.74	-0.45	op	60	60	61	70	59	69	...	...	82	72	73
6158.19	(10)	10.74	-0.31	op	72	80	71	86	70	85	66	83	99	86	92
6453.64	(9)	10.74	-1.30	op	11	16	...	11	15	15	...	...	...	...	...
6454.48	(9)	10.74	-1.08	op	17	27	...	20	20	25	...	...	...	...	...
7156.80	(38)	12.73	0.27	op	...	31	30	...	...	...	...	...	16	22	25

[a] Full designation for this multiplet in the Revised Multiplet Table (RMT; Moore 1970) is No. 25.02.
[b] Spectral line originates from two multiplets, RMT Nos. 26 and 25.02.

dance. The atmospheric parameters adopted for each star (see Venn 1995) are also listed in Table 2.

The estimated abundance uncertainties due to the temperature and gravity assignments per species are listed in Table 3. Uncertainties are shown for only six stars which represent a small subgroup of the program stars with similar atmospheric parameters and, thus, elemental abundance uncertainties, e.g., the abundance uncertainties for HD 87737 are similar to those for HD 46300, 161695, 175687, 195324, and 207673. The groups are listed at the bottom of the table. Only weak lines have been used to calculate the final abundances, therefore the uncertainties due to microturbulence (± 1 km s^{-1}) are less than 0.1 dex (the weak line criterion defined above).

4.1. *LTE Abundance Results*

The mean abundances determined here for the A-type supergiants are listed in Table 2 and shown schematically in Figure 2 relative to solar. The adopted solar abundances for comparison purposes are as follows; for oxygen, we adopt the photospheric abundance discussed by Anders & Grevesse [1989, log $\epsilon(O)_\odot = 8.93$], and for carbon and nitrogen we adopt the photospheric abundances from Grevesse et al. [1991, log $\epsilon(C)_\odot = 8.60$; 1990, log ϵ $(N)_\odot = 8.00$]. We adopt the meteoritic abundance for iron from Anders & Grevesse [1989, log $\epsilon(Fe)_\odot = 7.51$].

TABLE 1B

SPECTRAL LINE EQUIVALENT WIDTHS

λ	Mult.	χ	Log gf	Ref.	210221	67456	59612	34578	147084	148743	58585	25291	196379	36673	6130
C I:															
5380.24	(11)	7.68	-1.60	op	...	...	...	44	52	...	...	...	...	...	...
6001.13	(26.07)	8.64	-2.02	op	...	...	...	8:	...	...	...	15	...	...	16
6007.18	(26.07)	8.64	-2.02	op	...	...	...	6:	...	...	...	11	...	...	13
6010.68	(26.07)	8.64	-1.90	op	...	...	...	...	...	...	...	13	...	...	20
6012.24	(26.06)	8.64	-1.96	op	...	...	...	...	...	...	...	10	...	...	13
6013.22	(26.06)[a]	8.65	-1.11	op	...	30:	...	31:	...	...	...	56	...	...	59
6014.84	(26.07)	8.64	-1.55	op	...	...	...	13:	...	...	...	23	...	...	28
6587.75	(22)	8.54	-1.02	op	...	...	...	41	...	...	...	...	...	...	70
7100.12	(26.02)	8.64	-1.47	op	...	...	...	...	...	28	...	...	...	...	29
7108.94	(26.02)	8.64	-1.60	op	...	12	7	14	15	22	21	25	33	18	22
7111.48	(26)	8.64	-1.07	op	12	32	14	25	30	36	42	49	65	35	47
7113.18	(26)	8.65	-0.76	op	25	59	35	52	54	69	65	77	103	59	75
7115.19	(26)[a]	8.64	-0.92	op	20	51	33	48	53	67	68	78	101	59	76
7116.99	(25)[b]	8.65	-0.91	op	26	56	34	49	53	69	69	80	104	60	77
7119.67	(25)[b]	8.64	-1.15	op	15	40	23	33	37	37	46	53	68	36	62
9061.48	(3)	7.48	-0.34	op	...	...	...	*349*	...	...	*362*	*443*	...	...	...
9062.53	(3)	7.48	-0.45	op	...	...	...	*335*	...	...	*350*	*425*	...	...	...
9078.32	(3)	7.48	-0.58	op	*234*	*300*	...	*291*	...	*369*	*317*	*375*	...	*360*	*386*
9088.57	(3)	7.48	-0.42	op	*263*	*341*	...	*323*	...	*444*	*356*	*416*	...	*390*	*437*
9094.89	(3)	7.49	0.16	op	*410*	*447*	...	*449*	...	*592*	*469*	*530*	...	*540*	*521*
9111.85	(3)	7.49	-0.29	op	*289*	*353*	...	*341*	...	*482*	*368*	*429*	...	*421*	*440*
N I:															
7423.63	(3)	10.33	-0.69	zhu	124	87	150	91	107	125	102	...	...	...	...
7442.28	(3)	10.33	-0.40	zhu	179	90	179	115	125	152	107	93	53	*161*	92
7468.29	(3)	10.34	-0.21	zhu	*230*	115	*222*	*143*	*146*	196	129	118	61	*192*	106
8184.80	(2)	10.33	-0.29	zhu	...	...	...	114	...	*210*	...	97	...	*204*	112
8187.95	(2)	10.33	-0.29	zhu	...	...	...	139	...	*221*	...	110	108	*185*	*150*
8200.31	(2)	10.33	-1.00	zhu	...	...	...	...	...	...	...	...	...	...	...
8210.64	(2)	10.33	-0.68	zhu	...	...	...	86	...	131	...	75	50:	122	95
8216.28	(2)	10.34	0.09	zhu	...	...	...	*204*	...	*295*	...	*171*	117	*268*	*209*
8223.07	(2)	10.33	-0.29	zhu	...	...	...	131	...	185	...	121	74	*193*	130
8242.34	(2)	10.34	-0.26	zhu	...	...	...	*145*	...	191	...	116	59	*204*	*148*
8629.24	(8)	10.69	0.08	zhu	*262*	*133*	*260*	...	...	*247*	...	...	82	...	*139*
8703.24	(1)	10.33	-0.34	zhu	*287*	*136*	*274*	...	...	*259*	...	...	80	...	*144*
8711.69	(1)	10.33	-0.24	zhu	*310*	*146*	*293*	...	...	*284*	...	...	139	...	*163*
8718.82	(1)	10.34	-0.35	zhu	*266*	*147*	*261*	...	...	*253*	...	...	112	...	...
8728.88	(1)	10.33	-1.04	zhu	112	...	144	...	...	...	...	...	...	...	...
O I:															
6155.99	(10)	10.74	-0.67	op	50	49	51	46	40	50	47	...	...	...	...
6156.78	(10)	10.74	-0.45	op	92	56	75	69	57	78	62	52	...	64	55
6158.19	(10)	10.74	-0.31	op	110	84	96	85	70	104	80	...	96	103	97
6453.64	(9)	10.74	-1.30	op	22	...	...	...	...	20:	...	16	...	15	8:
6454.48	(9)	10.74	-1.08	op	46	22	...	...	...	28	...	19	...	20	10
7156.80	(38)	12.73	0.27	op	...	20	19	18	18	...	17	7:	19	11	10:

[a] Spectral line originates from two multiplets: λ6013.22 from RMT Nos. 26.06 and 26.07 and λ7115.19 from RMT Nos. 26 and 25.02.
[b] Full designation for this multiplet is RMT No. 25.02.

Carbon abundances have been determined primarily from two multiplets; λλ9100 in the hotter stars and λλ7115 in the cooler stars. Whenever possible, other multiplet lines were observed, but this was usually only in the cooler stars. Both of these spectral regions required the removal of telluric features which often slightly degraded the signal-to-noise ratio. The carbon abundances are in good agreement between multiplets and are in rough agreement from star to star, with an average underabundance of $[C/Fe\ II] = -0.14 \pm 0.20$. When the carbon abundances are plotted relative to temperature, the hottest stars in the program tend to have lower abundances than the cooler stars, as if there is a discontinuity near 9000 K (see Fig. 3). There may also be a slight increase in the carbon abundances with temperature from 7400 to 8500 K in the higher luminosity stars (Ib–Ia). These patterns may not be significant, but we shall return to discuss them after our NLTE analysis of carbon. No significant trends are found in the carbon abundances with gravity (see Fig. 4), except possibly for the F0 supergiants.

Nitrogen abundances have been determined from several multiplets. The lines near 7450 Å proved to be very useful because they are clean of blends through most of the tem-

TABLE 2

LTE Elemental Abundances

HD	Sp.Ty	T_{eff} (K)	Log g	ξ (km s^{-1})	C I log ϵ $\pm\sigma$ (#)	N I log ϵ $\pm\sigma$ (#)	O I log ϵ $\pm\sigma$ (#)
161695	A0 Ib	9950	2.2	3.0	8.24 ±0.05 (4)	8.92 ±0.22 (5)	8.89 ±0.06 (5)
87737	A0 Ib	9700	2.0	4.0	8.34 ±0.07 (5)	9.01 ±0.10 (3)	8.97 ±0.05 (6)
46300	A0 Ib	9700	2.1	4.0	8.16 ±0.10 (5)	8.66 ±0.18 (12)	8.87 ±0.05 (4)
175687	A0 II	9400	2.3	3.0	8.16 ±0.13 (3)	9.13 ±0.27 (3)	8.83 ±0.04 (5)
207673	A2 Ib	9300	1.75	5.0	8.39 ±0.11 (5)	8.86 ±0.10 (3)	8.85 ±0.06 (5)
195324	A1 Ib	9300	1.9	5.0	8.39 ±0.07 (3)	8.92 ±0.11 (5)	8.90 ±0.02 (5)
3940	A1 Ia	9200	1.4	6.0	7.80 ±0.06 (3)	8.62 ±0.14 (7)	8.77 ... (1)
14489	A2 Ia	9000	1.4	8.0	7.93 ±0.19 (4)	8.92 ±0.07 (2)	8.83 ... (1)
222275	A3 II	8500	2.2	3.0	8.63 ±0.15 (10)	9.28 ±0.07 (2)	8.91 ±0.06 (4)
13476	A3 Iab	8400	1.2	8.0	8.47 ±0.15 (5)	8.76 ±0.11 (4)	8.73 ±0.12 (4)
15316	A3 Iab	8350	1.2	7.0	8.50 ±0.23 (4)	8.68 ±0.18 (8)	8.73 ±0.02 (4)
34578	A5 II	8300	1.85	4.0	8.56 ±0.10 (12)	8.53 ±0.24 (6)	8.73 ±0.07 (4)
67456	A5 II	8300	2.5	3.0	8.42 ±0.09 (7)	8.76 ±0.13 (3)	8.80 ±0.08 (5)
147084	A5 II	8300	2.0	4.0	8.56 ±0.08 (7)	8.92 ±0.08 (2)	8.64 ±0.01 (4)
210221	A3 Ib	8200	1.3	7.0	8.39 ±0.09 (5)	8.88 ±0.10 (3)	8.88 ±0.14 (5)
59612	A5 Ib	8100	1.45	7.0	8.37 ±0.11 (6)	8.96 ±0.07 (3)	8.68 ±0.03 (4)
58585	A8 II	8000	1.8	4.0	8.52 ±0.09 (6)	8.74 ±0.13 (3)	8.68 ±0.04 (4)
148743	A7 Ib	7800	1.15	8.0	8.65 ±0.11 (7)	8.51 ±0.25 (6)	8.72 ±0.08 (5)
25291	F0 II	7600	1.5	4.0	8.41 ±0.09 (12)	8.25 ±0.19 (7)	8.54 ±0.22 (4)
196379	A9 II	7500	1.6	5.0	8.45 ±0.08 (6)	7.85 ±0.23 (11)	8.79 ±0.05 (2)
36673	F0 Ib	7400	1.1	4.0	8.14 ±0.08 (6)	8.46 ... (1)	8.68 ±0.17 (5)
6130	F0 II	7400	1.5	4.0	8.31 ±0.11 (14)	8.36 ±0.11 (5)	8.54 ±0.23 (5)
$\langle \log\epsilon_* \rangle$					8.35 ±0.21 (22)	8.72 ±0.32 (22)	8.77 ±0.12 (22)
$\log\epsilon_\odot$					8.60	8.00	8.93

Note.—The atmospheric parameters are those found and discussed in detail by Venn 1995.

perature range (with the exception of the coolest stars where N I λ7423 is blended with Si I). The wings of the Paschen lines near 8700 Å make some lines from multiplet No. 1 unusable. Telluric divisions near 8200 Å had to be done very carefully to recover the spectral lines with good signal-to-noise ratio. For the abundance analysis of the lines near 8200 Å, we found that the default continuum frequency sampling grid in WIDTH was too coarse for accurate abundances. When we refined the grid to calculate the continuum flux more carefully in this region where the Paschen jump occurs (8203.6 Å), then the abundances from these lines were in much better agreement with those from LINFOR calculations and with abundances from other multiplets.

Nitrogen is significantly overabundant in all the A-type supergiants, with [N/Fe II] ranging from 0.3 to 1.3 (only HD 196379 is not noticeably overabundant). These nitrogen enrichments are clearly related to T_{eff}, as shown in Figure 3. This trend strongly suggests the presence of a systematic error

TABLE 3A

Abundance Uncertainties

Element	87737		14489		13476	
	ΔT_{eff} +200K	ΔLog g +0.2	ΔT_{eff} +200K	ΔLog g +0.2	ΔT_{eff} +200K	ΔLog g +0.2
C I	+0.09	−0.07	+0.10	−0.14	+0.11	−0.16
N I	+0.07	−0.10[a]	+0.08	−0.09	+0.09	−0.07
O I	+0.03	−0.02	+0.05	−0.06	+0.05	−0.05

Note.—These uncertainties have been calculated specifically for the star at each column head. These uncertainties are representative of other program stars which have similar atmospheric parameters i.e., HD 87737 (46300, 161695, 175687, 195324, 207673), 14489 (3940), and 13476 (15316, 210221).

[a] Abundance uncertainties from HD 195324, 46300, and 175687 are smaller (−0.04).

TABLE 3B

Abundance Uncertainties

Element	34578		25291		36673	
	ΔT_{eff} +200K	ΔLog g +0.2	ΔT_{eff} +200K	ΔLog g +0.2	ΔT_{eff} +200K	ΔLog g +0.2
C I	+0.16	−0.08	+0.15	−0.03	+0.16	−0.05
N I	+0.04	−0.01	−0.01	+0.03	−0.02	+0.03
O I	+0.02	+0.01	−0.01	+0.02	+0.01	+0.05

Note.—These uncertainties have been calculated specifically for the star at each column head. These uncertainties are representative of other program stars which have similar atmospheric parameters i.e., HD 34578 (147084, 59612, 67456, 222275), 25291 (6130, 58585, 196379), and 36673 (148743).

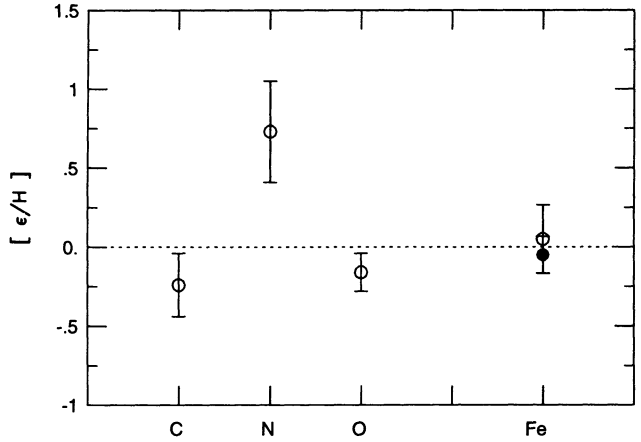

FIG. 2.—Mean LTE carbon, nitrogen, oxygen, and iron (from Venn 1995) abundances are plotted relative to solar (*dotted line*). The filled circle represents Fe II, while the unfilled circles represent abundances from neutral species.

in these nitrogen abundances that is not seen in the analysis of other elemental species; we shall return to this after our NLTE anaysis of nitrogen. We do not see any significant relationships in the nitrogen abundances with gravity (see Fig. 4), with the possible exception of the F0 supergiants. As a precaution, we also tested the effects of the damping coefficients on the nitrogen and carbon abundances, even through the analysis was restricted to weak lines only; adjusting the radiative, Stark, and van der Waals broadening coefficients by a factor of 2 had no significant effects ($\Delta \log \epsilon < 0.02$).

Oxygen abundances have been determined primarily from the lines near 6157 Å, which are clean and resolved through most of the atmospheric parameter range of this paper. Additional lines near 6454 Å were observed whenever possible. The average oxygen abundance is $[\mathrm{O/Fe\ II}] = -0.05 \pm 0.11$. There may be a slight rise in the oxygen abundances with temperature as seen in Figure 3, or the oxygen abundances from the hotter supergiants may be systematically higher (by $\sim$0.2 dex) than those from the cooler supergiants. This may indicate that departures from LTE are significant; we do not investigate the NLTE corrections to the oxygen abundances in this paper, other than to note that Baschek, Scholz, & Sedlmayr (1977) have estimated that LTE O I W_λ's may be 50% larger than NLTE W_λ's for a theoretical oxygen abundance in an A0-type supergiant atmosphere. These results are uncertain since the NLTE models used were very simplistic, but as a test, if we were to reduce our O I W_λ's for HD 87737 (A0 Ib) and HD 25291 (F0 II) by 30%, then the oxygen abundances would be reduced by $\sim$0.2 and 0.1 dex, respectively. This would bring the abundances from the hotter and cooler supergiants into marginally better agreement, suggesting that the slight trend we see may be a NLTE effect. Finally, no significant trends in the oxygen abundances with gravity are noticed (see Fig. 4).

4.2. *Comparison to Other Analyses*

We can compare the abundances derived for some of our program stars to those from other LTE analyses, i.e., for HD 36673, 148743, 87737, and 175687.

Luck & Lambert's (1985, hereafter LL) examination of HD 36673 (α Lep) includes atomic data and W_λ's that are in excellent agreement with ours (typically less than 10% difference for lines in common); thus, the derived abundances are also in good agreement after considering differences in the atmospheric parameters. There are only a few exceptions: first, the two O I lines near 6454 Å which are weak, and possibly slightly blended with strong Ca II and Fe II neighbors. These lines can be very difficult to measure if the resolution and signal-to-noise ratio are not excellent. They find W_λ's for these weak lines that are almost 2 times larger than our values; these W_λ's would increase the abundance we derive by $\sim$0.3 dex from these lines, which would make these line abundances quite discordant with the other multiplet lines. Second, their [C I] λ8727 line yields a rather large abundance (8.44), but this line is severely blended with N I and Si I lines. Their lower carbon abundance from λ5380 (7.90) is in agreement with what we find from the

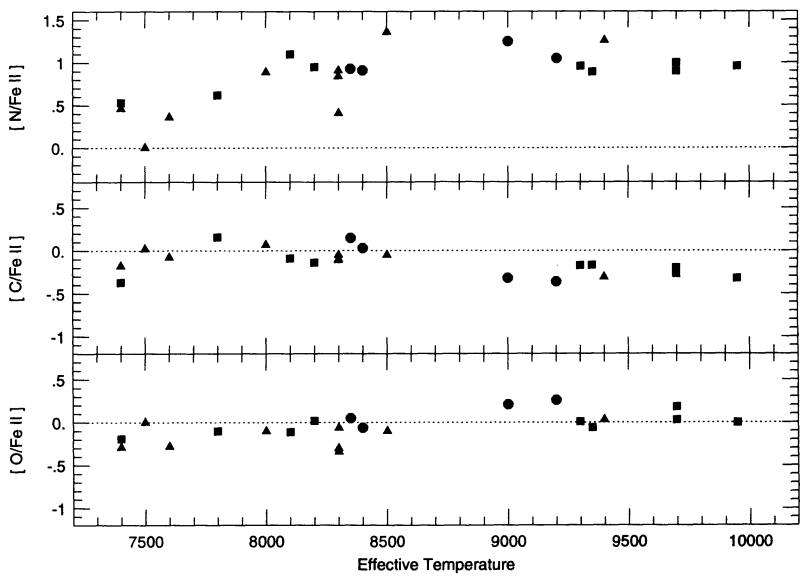

FIG. 3.—LTE CNO abundances relative to Fe II are plotted per star with respect to temperature. There is a strong correlation between the nitrogen abundance and temperature, but only slight relationships between the carbon and oxygen abundances with temperature. Differences in luminosity are noted (Ia and Iab stars appear as filled circles, Ib stars as filled squares, and II stars as filled triangles), but there are no significant deviations from the overall trends for these subgroups.

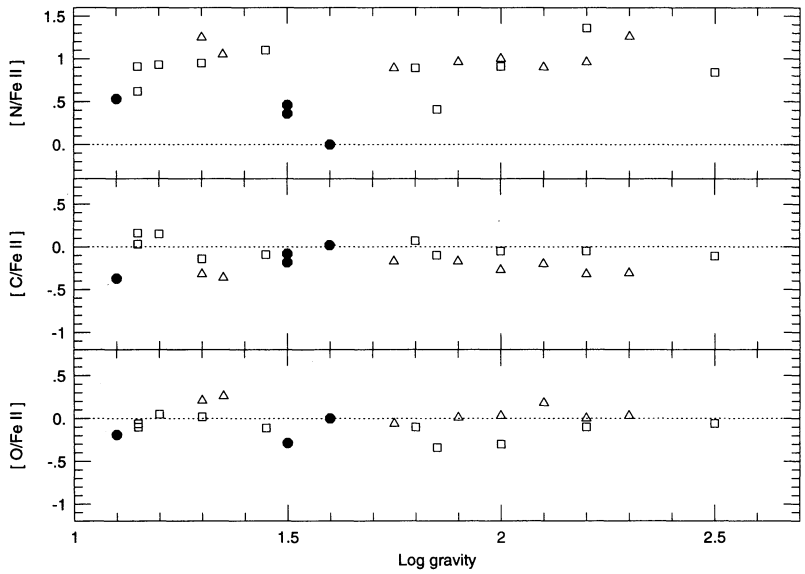

FIG. 4.—LTE CNO abundances relative to Fe II are plotted per star with respect to gravity. No correlations are found unless we look at small ranges in temperature; then, the cooler, A9–F0 stars (*filled circles*) may show some slight dependences. Other small ranges in temperature show no relation to gravity, including A0–A2 stars (*unfilled triangles*) and A3–A8 stars (*unfilled squares*).

$\lambda\lambda$7115 multiplet after correcting the atmospheric parameters. For nitrogen, LL were the first to show that NLTE effects are significant and based their nitrogen abundances on only the weakest line in their syntheses, λ8728.9. Unfortunately, this is the line that is severely blended with the forbidden C I line above and a Si I line. Therefore, the abundance from this line is probably overestimated, even without considering departures from LTE. They apply a correction of -0.2 dex to their N I abundance to try to account for NLTE effects, yet still find [N/H] = +0.66. Our calculation is from a clean, weak line of N I at 8210.6 Å; the LTE abundance is less than LL's LTE and NLTE results (we find [N/H] = +0.46).

Russell & Bessell (1989) have also analyzed the spectrum of HD 36673. We find the W_λ's are in agreement (to within 10%) for roughly two-thirds of the lines common to both analyses. However, the atmospheric parameters that they adopted for this star result in an abundance pattern that is quite different from the other A-type supergiants in our analysis and from the other four Galactic standard stars in theirs; in particular, carbon looks too depleted and sodium is roughly solar. Their other Galactic standards have abundance patterns more similar to our other A-type supergiants, where carbon is only slightly underabundant and sodium is quite overabundant (as found in Venn 1995). Thus, the unique abundance pattern they found for this star is probably an artifact of inappropriate atmospheric parameters. Finally, Spite & Spite (1990) used HD 36673 as a Galactic standard for an analysis of S/O and C/O in SMC supergiants. Our sulphur abundance for HD 36673 is higher than they have determined, due to differences in the atmospheric parameters. Our oxygen abundance is in good agreement with their mean value, but even considering differences in the atmospheric parameters, we find a much smaller carbon abundance.

It is important to compare our data set for HD 148743 (HR 6144) to that from Luck et al. (1990) for one particular reason, they conclude that HD 148743 has a chemical abundance pattern that is "strongly atypical of Population I supergiants" based on their results that [Fe/H] ~ -0.4, that CNO are all overabundant, and that the alpha elements appear enriched. But, using the new atmospheric parameters we have found, we find [Fe/H] is roughly solar, CNO resemble the abundances of the other A-type supergiants in this analysis, and the alpha elements have roughly normal abundances relative to iron. There is nothing in our analysis that distinguishes this star from the other normal A-type supergiants based on chemical composition, thus HD 148743 does *not* possess an atypical abundance pattern.

For HD 87737 (η Leo), the nitrogen and oxygen abundances derived by Lambert et al. (1989) are similar to ours after considering differences in the atmospheric parameters. Our carbon abundance is much smaller than theirs (by $\sim$0.4 dex), but they report only an upper limit based on marginal detections of C I lines near 7115 Å. We do not detect these lines in our spectra (see Fig. 1).

HD 175687 (ξ^1 Sgr) has recently been examined by Tomkin & Lambert (1994) as a comparison star for the secondary of an eclipsing binary system, V356 Sgr. Their atmospheric parameters are determined from Strömgren colors only, but are in fair agreement with the values we have determined with the exception of microturbulence (they adopt a value of 5 km s^{-1}, whereas we have found a value of 3 km s^{-1}). Several of the same spectral lines of C I, N I, and O I have been observed with most W_λ's in excellent agreement. The exceptions are two C I lines where Tomkin & Lambert find one value that is larger than ours and one that is smaller, each by $\sim$30%; it is not clear why these W_λ values differ by so much. As a result the nitrogen, oxygen, and iron abundances that they determine are in good agreement with ours, but their carbon abundance is larger (by $\sim$0.25 dex).

5. NLTE ANALYSIS OF CARBON AND NITROGEN

NLTE line formation calculations that use line-blanketed, LTE model atmospheres are employed; I. Hubeny would classify this as a "restricted" NLTE analysis. Our final NLTE carbon and nitrogen abundances are listed in Table 4.

TABLE 4

NLTE Carbon and Nitrogen Abundances

HD	[C/H] $\pm\sigma$ (#)	Δ[a]	[N/H] $\pm\sigma$ (#)	Δ[a]	[N/C] $\pm\sigma$	[N/C]$^{b}_{toB*}$	[Fe II]	[C/Fe]	[N/Fe]	[C+N]$^{c}_{toB*}$
222275	−0.25 ±0.17 (10)	−0.28	+0.31 ±0.25 (6)	−0.97	0.56 ±0.33	0.42	0.08	−0.33	0.23	0.17
13476	−0.55 ±0.16 (4)	−0.42	−0.04 ±0.08 (9)	−0.80	0.51 ±0.23	0.37	−0.12	−0.43	0.08	0.05
15316	−0.48 ±0.23 (4)	−0.38	−0.04 ±0.12 (12)	−0.72	0.44 ±0.33	0.30	−0.25	−0.23	0.21	0.22
34578	−0.34 ±0.11 (12)	−0.30	−0.03 ±0.14 (9)	−0.56	0.31 ±0.21	0.17	0.03	−0.37	−0.06	0.03
67456	−0.43 ±0.07 (7)	−0.25	+0.06 ±0.22 (7)	−0.70	0.49 ±0.27	0.35	−0.07	−0.36	0.15	0.11
147084	−0.36 ±0.09 (7)	−0.32	+0.23 ±0.12 (3)	−0.69	0.59 ±0.18	0.45	0.01	−0.37	0.22	0.17
210221	−0.61 ±0.09 (5)	−0.40	+0.19 ±0.04 (4)	−0.69	0.80 ±0.25	0.66	−0.07	−0.54	0.26	0.09
59612	−0.61 ±0.11 (6)	−0.38	+0.29 ±0.12 (4)	−0.67	0.90 ±0.29	0.76	−0.14	−0.47	0.43	0.23
58585	−0.41 ±0.10 (6)	−0.33	+0.16 ±0.16 (3)	−0.58	0.57 ±0.22	0.43	−0.15	−0.26	0.31	0.25
148743	−0.34 ±0.12 (7)	−0.39	−0.01 ±0.19 (9)	−0.52	0.33 ±0.24	0.19	−0.11	−0.23	0.10	0.18
25291	−0.43 ±0.11 (12)	−0.24	−0.15 ±0.11 (8)	−0.40	0.28 ±0.19	0.14	−0.11	−0.32	−0.04	0.07
196379	−0.41 ±0.08 (6)	−0.26	−0.43 ±0.20 (11)	−0.28	−0.02 ±0.26	−0.16	−0.17	−0.24	−0.26	0.07
36673	−0.71 ±0.09 (6)	−0.25	+0.30 ±0.13 (8)	−0.16	1.01 ±0.20	0.87	−0.08	−0.63	0.38	0.14
6130	−0.45 ±0.18 (14)	−0.16	−0.02 ±0.12 (11)	−0.38	0.43 ±0.25	0.29	−0.11	−0.34	0.09	0.10
$\langle[X]\rangle_{14}$	−0.46	−0.31	+0.06	−0.58	+0.51	+0.37	−0.09	−0.37	+0.15	0.13
$\pm\sigma_{14}$	±0.13	±0.08	±0.21	±0.22	±0.27	±0.27	±0.09	±0.12	±0.18	±0.07
161695	*−0.71 ±0.09 (4)*	*−0.35*	+0.03 ±0.11 (10)	−0.89	*0.74 ±0.18*	*0.60*	−0.04	*−0.67*	0.07	*−0.15*
87737	*−0.66 ±0.06 (6)*	*−0.40*	+0.09 ±0.06 (8)	−0.92	*0.75 ±0.12*	*0.61*	0.01	*−0.67*	0.08	*−0.07*
46300	*−0.81 ±0.08 (6)*	*−0.37*	−0.15 ±0.10 (15)	−0.81	*0.66 ±0.18*	*0.52*	−0.24	*−0.57*	0.09	*−0.02*
175687	*−0.80 ±0.14 (4)*	*−0.36*	+0.29 ±0.07 (4)	−0.84	*1.09 ±0.19*	*0.95*	−0.13	*−0.67*	0.42	*0.16*
207673	*−0.74 ±0.10 (6)*	*−0.53*	+0.04 ±0.04 (13)	−0.82	*0.78 ±0.14*	*0.64*	−0.01	*−0.73*	0.05	*−0.11*
195324	*−0.71 ±0.07 (4)*	*−0.50*	+0.14 ±0.10 (14)	−0.78	*0.85 ±0.15*	*0.71*	−0.04	*−0.67*	0.18	*−0.01*
3940	*−1.30 ±0.07 (3)*	*−0.50*	−0.25 ±0.11 (10)	−0.87	*1.05 ±0.18*	*0.91*	−0.40	*−0.90*	0.15	*−0.10*
14489	*−1.20 ±0.18 (4)*	*−0.53*	+0.01 ±0.06 (6)	−0.91	*1.21 ±0.28*	*1.07*	−0.27	*−0.93*	0.28	*0.00*
$\langle[X]\rangle_{22}$	···	···	+0.05	−0.68	···	···	−0.11	···	+0.15	···
$\pm\sigma_{22}$	···	···	±0.19	±0.22	···	···	±0.11	···	±0.16	···

Note.—Values in italics are based on C I $\lambda\lambda$9100 lines, which we do not consider to be reliable abundance indicators. Also, all N I lines observed with equivalent widths $\leq$250 mÅ are included in the NLTE N abundance per star.

[a] Δ = NLTE − LTE mean values.

[b] $[N/C]_{to\ B*} = \log\epsilon(N/C)_{A1} - \log\epsilon(N/C)_{B*}$, where the mean B star abundances are [C/H] = −0.35 and [N/H] = −0.21 (see text).

[c] $[C + N]_{to\ B*} = \log\epsilon(C/Fe + N/Fe)_{A1} - \log\epsilon(C/Fe + N/Fe)_{B*}$, assuming $\log\epsilon(Fe)_{B*}$ is solar.

5.1. *Outline of the Calculations*

In LTE, the occupation numbers (n_i) of each atomic level (i) of an element are simply calculated from the Saha-Boltzmann equation using the *local* parameters at each atmospheric layer (e.g., $T_{\rm eff}$ and electron density). The added complexity of NLTE calculations is that the occupation numbers are also affected by the radiation field which is dominated by *nonlocal* conditions, i.e., global properties of the star. A NLTE solution for the statistical equilibrium of an element must account for all of the radiative and collisional processes populating and depopulating an atomic level at each atmospheric layer of the star. The result can be represented by a set of *departure coefficients* (defined as $b_i = n_{i\rm NLTE}/n_{i\rm LTE}$) for each atomic level. Departure coefficients for C and N in this analysis have been calculated using a system of codes developed by W. Steenbock at the University of Kiel. These codes use the *complete linearization* techniques introduced by Auer & Heasely (1976). Complete linearization is the method by which all physical properties in a stellar atmosphere (i.e., temperature, electron density, mean radiation field, elemental abundances, and elemental occupation numbers) are treated as individual, but equally important parameters that can interact globally.

The departure coefficients that are output from Steenbock's programs are in ready form to be used with the abundance code LINFOR to calculate NLTE abundance corrections. The same atmospheric parameters, including microturbulence values, determined from the LTE analysis of the metal lines in these stars are used for the carbon and nitrogen NLTE abundance analyses. There has been some suggestion that lower microturbulence values are found when NLTE effects are considered (e.g., Gies & Lambert 1992; Boyarchuk, Lyubimkov, & Sakhibullin 1985), but we did not find any significant evidence for this effect because our abundance analysis is based on weak lines which are not strongly affected by microturbulence.

5.2. *Carbon*

Departure coefficients for carbon have been calculated from an atomic model based on the data collected by Stürenburg & Holweger (1990, hereafter SH), and which was made available to us by S. Stürenburg. This model was designed to examine C in the Sun and Vega, where discrepancies between strong and weak line abundances were resolved. The model atom is very detailed, including 83 levels of C I, and all known terms up to principal quantum number $n = 7$, 0.26 eV below the ionization limit (11.26 eV). It also includes the five energetically lowest levels of C II up to excitation energy 13.72 eV. A total of 63 C I line transitions and three lines of C II are treated explicitly, where transition probabilities have been adopted from the literature, ignoring multiplet structure. A diagram for the SH model is shown in Figure 1 in Stürenburg & Holweger's paper, and we refer the reader to their paper for further atomic details.

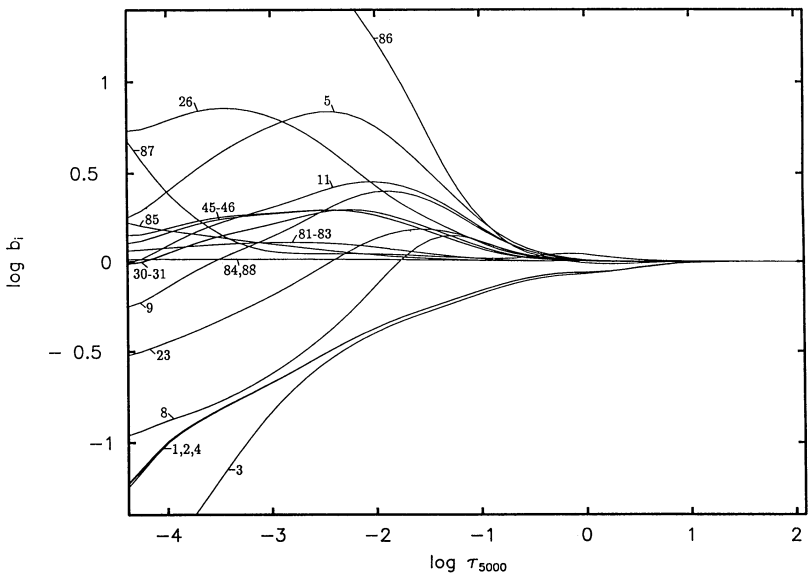

FIG. 5.—Departure coefficients of carbon for HD 13476 (A3 Iab). Levels have been labeled according to the numbering in SH. Note that levels 84 to 88 represent the lowest energy levels of C II.

5.2.1. *Application of the Carbon Model Atom to A-Type Supergiants*

NLTE calculations using SH's model atom showed that the level populations are quite different from those in LTE for the A supergiants. Departure coefficients for a selection of levels are shown in Figure 5 for HD 13476 (A3 Iab). In the line-forming region, C I is overionized from its LTE value in the A0–A7 supergiants, and the four energetically lowest levels of C I (designated as levels 1, 2, 3, and 4) are underpopulated relative to their LTE values due to strong radiative transitions to higher levels and the continuum. The underpopulations of the lowest levels are most severe in the hottest A0-type stars. The occupation numbers of several levels are overpopulated in the line-forming regions, although lower levels of observed transitions are less overpopulated than the upper levels, and NLTE corrections are negative.

In the A9–F0 supergiants, the departure coefficients for the four lowest levels of C I and the ground states of C II are close to their LTE values throughout the line-forming atmospheric layers. Radiative transition between bound-bound states cause very slight overabundances of the atomic levels of observed transitions in the line-forming regions, leading to negative NLTE abundance corrections, but with smaller values than in the hotter stars.

After applying the SH model atom, the LTE carbon abundances proved to be too large by $\sim$0.3 dex in the A3–F0 supergiants. The corrections to C in the A0–A2 supergiants are larger at $\sim$0.5 dex. The C corrections for these two groups of stars appear to be distinct from one another. As discussed earlier and shown in Figure 3, the LTE abundances of the cooler (7400–8500 K) stars rise slightly with increasing temperature, particularly for the higher luminosity stars; this rise is eliminated by the NLTE corrections, such that these NLTE carbon abundances show no significant trend with temperature. The abundances in these cooler stars are based on only weak lines that are from a variety of multiplets and atomic levels, where the NLTE corrections range from -0.1 to -0.5 dex. In the A0–A2 supergiants, the carbon abundances are calculated from only one multiplet, which results in extremely low NLTE C abundances that are discordant with the abundances from the cooler stars. This result is disturbing and suggests a significant change in the description and/or calculations of carbon (or at least of the sole multiplet being used) in the hotter stars. We shall investigate this further below.

5.2.2. *Uncertainties in the Carbon NLTE Abundances*

Numerous test calculations have been performed with the SH model atom to test the influence of the atomic data on the resultant NLTE abundances. The tests we have performed are summarized in Table 5 for three representative stars. The NLTE corrections for the carbon abundances are sensitive to changes in only a few pieces of the atomic model, particularly the collisional excitation cross sections. However, the NLTE corrections to the C I λ9100 multiplet cannot be affected by reasonable changes in the carbon model atom to force these lines to yield carbon abundances in the hotter stars that are in agreement with the abundances in the cooler stars.

1. The expected uncertainties in the *atmospheric parameters* for the LTE model atmospheres adopted have only small to moderate effects on the NLTE carbon abundances. In particular, since only weak lines of C I have been included in the NLTE abundances, small changes in ξ are not significant.

2. *Photoionization cross sections* were reduced by a factor of 10 for the five energetically lowest levels of C I, both individually and together. Changes to the first three levels showed some small effects on the abundance corrections ($\pm$0.04 dex), but when all five levels were changed simultaneously the change was negligible ($<$0.02 dex). Thus, reasonable uncertainties in the photoionization cross sections for the first five levels yield only small uncertainties in the departure coefficients. These are the only levels where photoionization has strong effects in the line-forming atmospheric layers. Overall, replacing the Hofsaess (1979) photoionization cross sections adopted by SH with those calculated by the OP causes the abundance corrections to be slightly smaller ($\sim$0.05 dex), but this is a systematic change affecting the A0 and F0 supergiants similarly.

TABLE 5

UNCERTAINTIES IN THE NLTE ANALYSIS OF CARBON

	$\Delta\log\epsilon(C)_{NLTE}$		
	HD 87737	13476	6130
1. $\Delta T_{\rm eff}$ = +200 K	(+0.09)	+0.14 (+0.16)	−0.01 (+0.04)
2. Δ log g = +0.2	(−0.02)	−0.10 (−0.09)	+0.08 (+0.02)
3. $\Delta\ \xi = -1$ km s^{-1}	(+0.03)	+0.01 (+0.06)	+0.02 (+0.37)
4. Photoionization Cross-sections:			
(a) Replace with OP X-sections	(+0.05)	+0.06 (+0.05)	+0.03 (+0.03)
(b) X-sections for Levels *1* to *5* * 0.10	(+0.02)	+0.06 (+0.07)	0.00 (0.00)
5. Line transitions f_{ij} * 0.333	(+0.05)	+0.08 (+0.05)	+0.04 (0.00)
6. Including All transitions of $\lambda\lambda$9100	(−0.09)	0.00 (−0.03)	0.00 (−0.22)
7. Additional line transitions from OP (total=242)	(−0.06)	−0.09 (−0.06)	+0.04 (0.00)
8. Collisional Ionization Cross-sections:			
(a) Replaced by Mihalas formulation	(+0.02)	0.00 (+0.01)	0.00 (0.00)
(b) Mihalas X-sections * 10.0	(0.00)	0.00 (0.00)	0.00 (0.00)
(c) Mihalas X-sections * 0.10	(+0.01)	0.00 (0.00)	0.00 (0.00)
9. Collisions with Neutral Particles = 5.0	(0.00)	0.00 (0.00)	+0.02 (+0.07)
10. Reduced $C_{\rm init}$	(−0.01)	0.00 (0.00)	0.00 (0.00)
11. Collisional Excitation Cross-sections:			
(a) All X-sections * 0.333	(−0.13)	−0.04 (−0.12)	0.00 (0.00)
(b) All Replaced by Auer & Mihalas formulations	(+0.07)	0.00 (+0.07)	+0.03 (+0.12)
(c) Replaced Rad.ly Perm. only by Auer & Mihalas form.	(+0.07)	+0.02 (+0.07)	+0.03 (+0.12)
(d) Replaced Rad.ly Forb. only by Auer & Mihalas form.	(0.00)	−0.02 (−0.01)	0.00 (−0.03)
(e) Rad.ly Permitted X-sections * 0.333	(−0.11)	−0.03 (−0.12)	−0.04 (−0.17)
(f) Rad.ly Forbidden X-sections * 0.10	(+0.12)	+0.10 (+0.09)	+0.03 (+0.08)
(g) Rad.ly Forbidden X-sections * 10.0	(−0.03)	−0.02 (−0.02)	−0.01 (−0.01)

NOTE.—Uncertainties are calculated for the mean of the carbon abundances, excluding the strong λ9100 multiplet lines (mean abundances from these lines are shown in brackets).

3. Reducing the *line strengths* by a factor of 3 to mimic uncertain *f*-values had only a small effect on the NLTE corrections (~0.05 dex). A test that replaces Stürenburg's line transitions (which are the wavelengths and *f*-values of the strongest lines in the multiplets) with multiplet values from the OP proved to have no significant effect on the depature coefficients. An additional 188 multiplet lines (with $\lambda < 15000$ Å) were added to the model atom with only marginal effects on the departure coefficients in the line-forming regions. When lines are removed from the model atom, there can be substantial changes in the abundance corrections since the departure coefficients of the energetically middle levels are dominated by bound-bound transitions (particularly transitions out of the ground state). This emphasizes the importance of including many transitions, particularly from the low lying levels, for reliable NLTE carbon abundance corrections.

4. *Neutral particle collision rates* were increased from $\frac{1}{3}$ to 5 times the values of the electron collision cross sections (as suggested in Tomkin et al. 1992), but had no significant effect on the NLTE corrections (as expected at these temperatures). Also, changes in the *collisional ionization rates* had only negligible effects on the NLTE abundances.

5. The *initial C abundance* was reduced to the NLTE carbon abundance determined after preliminary calculations. Since C I is an important background opacity source, particularly in the UV where strong bound-free transitions from the ground state can contribute to the background opacity, the initial carbon abundance can affect the radiation field, which will affect the statistical equilibrium results of carbon itself. Yet, no significant differences in the NLTE abundances were found.

6. *Electron collisional excitation rates* were globally reduced by a factor of 3 which caused a significant increase in the NLTE corrections (~0.1 dex) for the hotter supergiants (as might have been predicted since this moves the statistical equilibrium further away from LTE), but had no effect on the cooler supergiants. This sort of effect could reduce or eliminate the difference in the NLTE carbon abundances between the hotter and cooler supergiants that we currently find, and so we investigate this further. Cross sections for the electron collisions have been calculated using the Drawin (1967) formulae,

with maximum cross sections calculated depending on the line strength (known or assumed). A test to further minimize the effects of electron collisions by setting all the electron collision cross sections to $0.01\pi a_0^2$ increased the NLTE corrections substantially in the A0 supergiants. These tests were performed on the allowed transitions (assuming *LS* coupling) and the forbidden transitions individually and together; individually, reducing either the forbidden or allowed cross sections increased the abundance corrections by 0.3 dex, and together they increase corrections by 0.4 dex such that the NLTE abundance in, for example, HD 87737 would be much less, $\sim$7.5 dex. This would put the C I abundances between the hotter and cooler supergiants even further apart. Thus, we also tried increasing all the cross sections to πa_0^2 to test the effects of maximizing the electron collision rates (moving the statistical equilibrium closer to LTE). This caused the NLTE corrections to become substantially reduced for the hotter stars (to only $\sim$0.2 dex), and nearly zero in the cooler stars (thus occupation numbers are near their LTE values). This would remove the difference in the NLTE abundances between the hotter and cooler stars almost completely, but applying this model to Vega causes the strong lines to have much larger NLTE abundances than the weak lines. Therefore, this does *not* appear to be a better (i.e., realistic) C I model, but it does show that the statistical equilibrium of carbon in these atmospheres is very sensitive to the collisional excitation cross sections.

We also examined replacing the collisional excitation cross sections with values calculated using the Auer & Mihalas (1973) formulae, which are also energy-dependent cross sections (two formulae are available depending on whether the transition is radiatively permitted or forbidden). We found a slight increase ($\sim$0.1) in the NLTE abundances calculated from the strong C I λ9100 lines, but almost no effect on the weaker lines from several other multiplets. Scaling these cross sections (to test the sensitivities of the NLTE corrections from these formulae) for forbidden transitions by a factor of 10 and for permitted transitions by a factor of 3, separately, caused additional changes in the NLTE corrections of $\sim$0.1 dex. But these scaling factors cause the strong lines in Vega to have systematically higher abundances than the weak lines, which is again *not* an improvement to the SH model. Thus, the NLTE carbon abundances in the A-type supergiants are sensitive to the adopted collisional excitation cross sections; however, reasonable changes in these to the SH model tend to cause only small changes in the calculated abundances, or to worsen the SH results for Vega.

7. After the tests described above, we closely examined the NLTE corrections for *the* λ9100 *multiplet lines* since these are the only C I lines observed in the A0–A2 supergiants. The C I lines near 9100 Å are observed throughout the temperature range of this analysis, but are too strong to be used in the A3–F0 supergiants. The λ9100 multiplet occurs between levels $3s^3P^0$ (level 5) and $3p^3P$ (level 11), which are both overpopulated in the line-forming regions in all the A-type supergiants. The lower level of this transition is unique in the NLTE calculations; level 5 is the most severely overpopulated C I level at all temperatures in these calculations and is only used in this analysis for the λ9100 multiplet NLTE corrections. Level 5 is slightly depopulated by photoionization (more so at hotter temperatures), but it is severely overpopulated by a strong radiative transition from the ground state (level 1). As a test, we reduced the *f*-value of this transition (at 1657 Å) by a factor of 10, which changed the NLTE corrections for the λ9100 lines by only $\leq$0.05 dex.

Next, we tried increasing the collisional coupling of the lowest four C I levels to level 5. The overpopulation of level 5 can be significantly decreased by this coupling since the lower levels are underpopulated by photoionization. Currently, the SH model uses the radiative transition *f*-value to calculate the collisional cross section between levels 1 and 5, but the radiative rates from levels 2, 3, and 4 are forbidden; therefore, the SH model uses a default lower limit of $0.01\pi a_0^2$ as the collision cross section. If we increase the collisional coupling to πa_0^2, the overpopulation of level 5 decreases such that the NLTE abundance correction is much smaller, only about -0.15 dex for the A0 supergiants. The NLTE C abundances would then be in agreement with those from the cooler stars. Collisionally coupling level 5 to the ground states is probably not realistic though, since the energy differences between level 5 and the lowest levels are quite large. Also, this causes the strong λ9100 lines (and other multiplet lines out of level 5) in Vega to have negligible NLTE corrections, and therefore the good agreement that the SH model yields between strong and weak line NLTE carbon abundances in Vega is no longer present.

The only possibly realistic way to bring the abundances from the λ9100 lines in the hotter stars into agreement with those from other C I multiplets in the cooler stars is to change the *f*-value of the λ9100 multiplet itself. If we decrease the *f*-value of this multiplet by a factor of 10, then the NLTE corrections are decreased by $\sim$0.2 dex in the hotter supergiants, but only $\sim$0.04 dex in the cooler stars and Vega (although we do not actually include the strong λ9100 lines in the NLTE abundances calculated for the cooler stars). This change in the C I atomic data is intriguing because the NLTE corrections to the strong λ9100 lines in Vega are still in agreement with Vega's weak line abundances. Unfortunately, however, the changes needed in the *f*-values are probably not warranted. The *f*-value for the λ9100 multiplet is estimated as accurate to within 0.05 dex (cf. Nussbaumer & Storey 1984). It may be possible that the change in the multiplet *f*-value is compensating for other effects that are poorly represented in our calculations, for example, uncertainties in (1) the model atmosphere, e.g., atmospheric structure changes due to neglected NLTE effects, or (2) the model atom, e.g., the model does not account for fine structure in calculating the level populations. It is also possible that (3) a stellar wind component could affect these lines, e.g., these lines form a little farther out in the atmosphere where a stellar wind might fill in the lines slightly, resulting in smaller equivalent widths, and thus lower abundances if it is ignored (which could even affect weak lines; cf. Kudritzki 1992), or perhaps (4) there is missing physics in the NLTE calculation. Therefore, at present, we must conclude that the NLTE abundances from the λ9100 lines appear to be unreliable. Omitting these lines from the abundance analysis means that we cannot calculate the C abundances in our sample of hotter, A0–A2, supergiants.

5.2.3. *Carbon NLTE Abundances (without the* λ*9100 lines)*

The average NLTE carbon abundance in the 14 A3–F0 supergiants in this analysis is $\log \epsilon(\mathrm{C/H}) = 8.14 \pm 0.13$, or $\langle[\mathrm{C/H}]\rangle = -0.46 \pm 0.13$. Relative to iron, this average is $\langle[\mathrm{C/Fe\ II}]\rangle = -0.37 \pm 0.12$, where $\langle[\mathrm{Fe\ II/H}]\rangle = -0.09 \pm 0.09$ for these 14 stars. The abundances per star are listed in Table 4. The average LTE C abundance for the 14 A3–F0 supergiants in this analysis was found to be $\log \epsilon(\mathrm{C/H}) = 8.45 \pm 0.13$ from the same (weak) spectral lines (with the exception of HD 13476, for which one line at 9078 Å was used in the LTE abundance, but was discounted for the NLTE

TABLE 6

NLTE Corrections for Carbon Line Abundances

λ	87737			13476			6130		
	W_λ	NLTE	Δlogϵ	W_λ	NLTE	Δlogϵ	W_λ	NLTE	Δlogϵ
$3p^3D - 5s^3P^o$:									
7100.12		...			...		29	8.08	−0.20
7108.94		...			...		22	8.08	−0.19
7115.19		...		10	7.87	−0.49	76	8.05	−0.24
7116.99		...		17	7.95	−0.64	77	8.05	−0.25
7119.67		...		10	8.18	−0.40	62	8.16	−0.22
$3p^3D - 4d^3F^o$:									
7111.48		...			...		47	7.92	−0.21
7113.18		...		12	8.18	−0.10	75	7.89	−0.24
$3s^3P^o - 3p^3P$:									
9061.48	90	7.94	−0.42		...			...	
9062.53	86	8.03	−0.41		...			...	
9078.32	58	7.94	−0.37	184	7.87	−0.70	386	7.92	−1.19
9088.57	82	7.97	−0.40	240	7.88	−0.77	437	7.99	−1.37
9094.89	175	7.90	−0.66	392	7.66	−1.08	521	7.84	−1.54
9111.85	81	7.84	−0.40	240	7.74	−0.77	440	7.89	−1.37
$3p^1P - 4d^1P^o$:									
6587.75		...			...		70	8.03	−0.20

Note.—The values for $\Delta \log \epsilon = \log \epsilon(C)_{NLTE} - \log \epsilon(C)_{LTE}$. We do not consider the C I λ9100 lines to yield reliable carbon abundances. For HD 6130, the lines observed near 6010 Å (not listed above) are quite weak, and thus have small abundance corrections, $\Delta \log \epsilon(C) \sim -0.10$.

abundance). Thus, the mean NLTE correction to the carbon abundance of A-type supergiants is −0.31 dex (±0.08 dex). NLTE abundance corrections for individual C I lines are listed in Table 6 for three representative stars.

The NLTE and LTE carbon abundances for all stars are plotted in Figure 6, where it can be seen that the marginal trend in the LTE abundances with temperature between 7400 and 8500 K is removed by the NLTE corrections. We also notice in this plot that the carbon NLTE corrections increase with temperature such that the *corrections* for the hottest supergiants (~9500 K) are consistent with what would be expected from the trend observed in the cooler stars. This would imply that the carbon NLTE *corrections* are, in fact, accurate for the λ9100 multiplet, but that the original LTE abundances are in error (perhaps too low by ~0.4 dex). Since we had tested the atomic data adopted for the initial LTE analysis for these C I lines (e.g., the multiplet *f*-value is estimated as accurate to within 0.05 dex—cf. Nussbaumer & Storey 1984—and the abundances from the multiplet lines were not especially sensitive to the radiative, Stark, and van

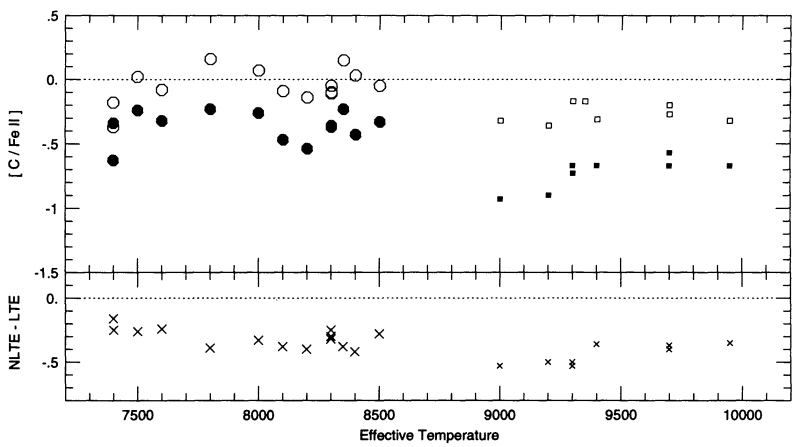

Fig. 6.—NLTE carbon abundances (*filled circles*) and LTE carbon abundances (*unfilled circles*) are shown for A3–F0 supergiants. The NLTE corrections (shown at bottom) are clearly temperature dependent, which removes the slight temperature dependence of the LTE abundances. For the hotter supergiants, NLTE carbon abundances (*small filled squares*) and LTE carbon abundances (*small unfilled squares*) are also shown. These abundances appear to be discordant with those from the cooler supergiants, which we presume is due to unrecognized problems in theoretically reproducing the C I λ9100 multiplet lines. However, notice that the NLTE corrections for the hotter stars are in agreement with the temperature trend of the A3–F0 supergiants.

der Waals broadening coefficients assumed), then perhaps departures from the classical, LTE model atmospheres that we have adopted significantly affect these lines. This possibility cannot be examined without line-blanketed NLTE model atmospheres which are currently not available, although we note that the λ9100 lines form fairly deep in the atmosphere ($\log \tau_{5000} \sim -0.7$) where LTE is usually a sufficient discription. Nevertheless, the abundances from these lines should be explicitly examined with NLTE model atmospheres in the future.

This is the first analysis of NLTE effects on carbon abundances in A–F supergiant stars, thus we cannot compare these results to other analyses. We conclude that NLTE effects do need to be considered for accurate carbon abundances in A0–F0 supergiants. For the continuing discussion of the evolutionary status of the A-type supergiants, it will be necessary to limit the discussion of the carbon abundances to only those for the A3–F0 supergiants for which reliable NLTE C abundances could be calculated.

5.3. *Nitrogen*

A new detailed nitrogen model atom has been built for these calculations and calibrated with respect to Vega by Lemke & Venn (1995). The model includes 88 levels of N I, 0.11 eV below the ionization limit of 14.53 eV, and five levels of N II up to 25.97 eV. This includes all known terms of N I up to principal quantum number $n = 8$ (Moore 1975). We include 189 radiative transitions explicitly, with f-values taken from the OP database. Multiplet structure was ignored, and each line is represented by a multiplet f-value. The model is shown in Figure 7, including only 101 transitions to clearly separate the doublet and quartet systems. Photoionization is taken into account for all 93 atomic levels; photoionization cross sections are from the OP database, and each transition is represented by 200–2000 frequency points.

Collisional coupling between each atomic level and all other levels and the continuum is taken into account. Collisional cross sections have been calculated using the formulae of Auer & Mihalas (1973). For permitted lines, the formula is based on the van Regemorter (1962) formula where a dipole approximation is assumed, and the f-value of the radiative transition and the energy difference between levels is used to calculate the collisional cross section. For radiatively forbidden transitions, a formula using a collision strength (Ω) and the energy difference between the levels is used; since we have no information on the collision strengths for N I, we have assumed $\Omega = 1.0$. Collisional ionizations are taken into account using the formula from Mihalas (1978, p. 134), which expresses a cross section in terms of the threshold photoionization cross section.

Calculations by Takeda (1992) showed the importance of metallicity in determining the nitrogen NLTE abundance in Vega (reexamined by Lemke & Venn 1995). We have found that this metallicity dependence is due primarily to the carbon abundance. This is because carbon bound-free transitions are a significant source of background opacity in the UV where photoionization of the N I ground states occurs. When a lower metallicity model is used (lower carbon abundance), then the UV flux is significantly higher, and photoionization of the N I

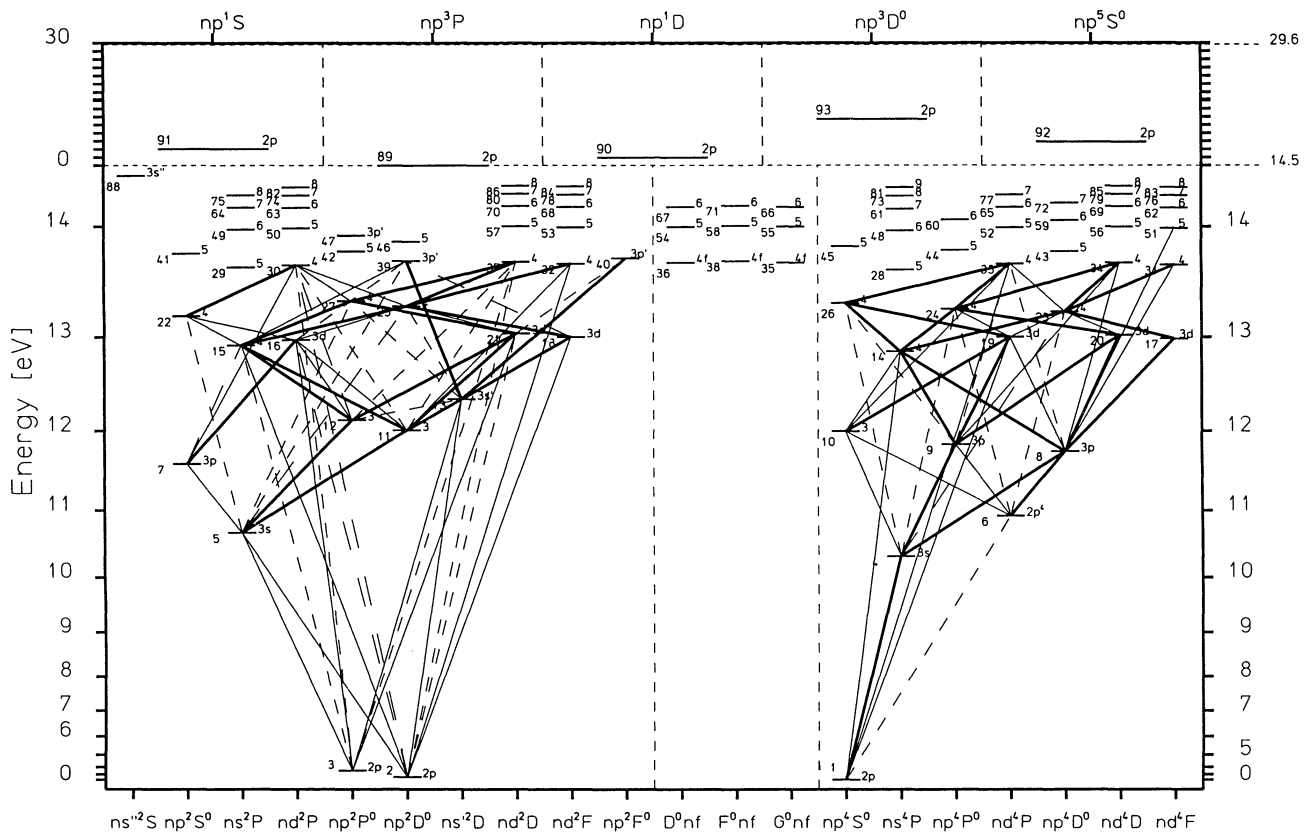

FIG. 7.—Diagram of the nitrogen model atom built by Lemke & Venn (1995). Term designations for the N I levels are marked on the bottom, for N II levels on the top. Strong line transitions are represented by thick solid lines, and the weakest transitions by thin short-dashed lines, with two degrees of strength in between.

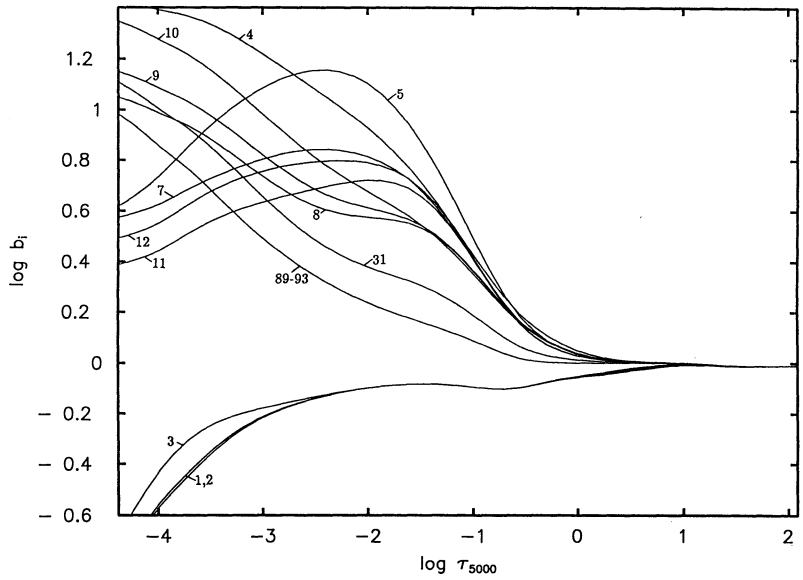

FIG. 8.—Departure coefficients of nitrogen for HD 13476 (A3 Iab) (also discussed in Table 8). Levels have been numbered according to Fig. 7 of the model atom. Note that levels 89 to 93 represent the lowest energy levels of N II.

ground states is greater, which affects the overall statistical equilibrium of the nitrogen atom. We also found that the carbon abundance has an effect on the NLTE nitrogen abundances calculated from doublet versus quartet system lines. For Vega, the abundances from doublet and quartet lines was improved by using its NLTE carbon abundance (vs. the slightly higher LTE abundance). Because of this effect, we have adopted our lower NLTE carbon abundances for the NLTE nitrogen calculations in this analysis.

5.3.1. *Application of the Nitrogen Model Atom to A-Type Supergiants*

When the N I atomic model is applied to the A-type supergiants, the N abundance corrections prove to be very large and temperature dependent, reducing the LTE N enrichments and completely removing the trend in the LTE abundances with temperature. Departure coefficients for HD 13476 (A3 Iab) are shown in Figure 8.

Photoionization is the most important atomic process determining the populations of the three lowest levels of N I in A-type supergiants, causing them to be underpopulated in the line-forming atmospheric layers for all the A0–F0 supergiants. The carbon abundance is also an important parameter (as found from our Vega calibrations); when the C abundance is lowered [to the values found from our C NLTE analysis for the A3–F0 stars, and log ϵ(C) = 8.20 for the A0–A2 stars], then the occupation numbers of the lowest three levels are further decreased. Photoionization slightly overpopulates the energetically middle levels of N I in the line-forming atmospheric region, but bound-bound radiative transitions from the ground states are more significant in substantially overpopulating these levels. The doublet and quartet systems react differently to changes in the carbon abundance, which is a useful test for the nitrogen results (since the doublet and quartet radiative transitions should yield the same NLTE abundances).

After applying the nitrogen model atom to the A-type supergiants, the LTE abundances proved to be too large by 0.2–1.0 dex. The corrections are related to temperature such that the hotter supergiants have the largest corrections. The hotter supergiants also have the largest LTE abundances, such that the final NLTE abundances are independent of temperature as shown in Figure 9.

5.3.2. *Testing the Nitrogen Model Atom and NLTE Abundances*

Numerous tests have been done to determine the accuracy of the nitrogen NLTE corrections due to possible errors in the atomic and atmospheric data and are summarized in Table 7.

1. The expected uncertainties in the *atmospheric parameters* yield only small to moderate differences in the NLTE calculations.

2. Using a solar carbon abundance instead of the *lower* C *abundances* determined from our NLTE analysis has only a small effect ($\sim$0.1 dex) on the NLTE nitrogen abundances. But the higher carbon abundance tends to cause larger discrepancies between the doublet and quartet line abundance results.

3. We tested the effect of uncertainties in the *photoionization cross sections* by reducing them by a factor of 10 for the three lowest levels. Changes in the abundance corrections were negligible for the cooler stars (where photoionization is not a strong effect), but were more significant in the hotter supergiants, causing the three lowest levels to be more depleted in the line-forming atmospheric layers. We also tried replacing the photoionization rates with the descriptions from Hofsaess's (1979) calculations to test the sensitivity of the very detailed values that we adopted, but this caused only a marginal change in the NLTE abundances which was systematic for all the supergiants.

4. The multiplet *f*-values adopted for the *line transitions* were globally reduced by a factor of 3 to mimic inexact values. The resulting changes in the NLTE abundances range from +0.05 in the cooler supergiants to +0.15 in the hotter stars. An additional 325 lines from the OP (with $\lambda < 15000$ Å) were added to the model atom, each representing a single multiplet. The effect was a negligible difference in the NLTE correction; therefore, our model appears to have a sufficient number of lines. We also tested the model with fewer lines, e.g., including only the 24 lines in LL's pioneering N I model. The NLTE abundances become much larger, by $\sim$0.25 dex in the hotter supergiants and $\sim$0.1 dex in the cooler stars. This test does not

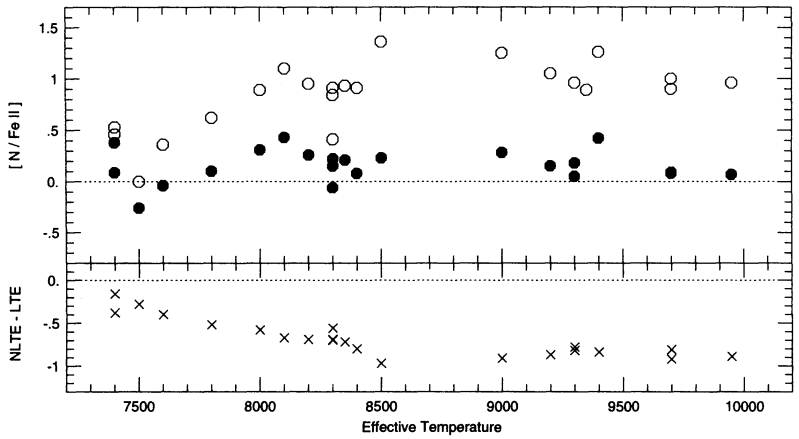

FIG. 9.—NLTE nitrogen abundances (*filled circles*) and LTE nitrogen abundances (*unfilled circles*) are shown for the 22 A-type supergiants analyzed. The NLTE corrections shown at the bottom are clearly temperature dependent and remove the temperature dependence of the LTE abundances. The mean NLTE nitrogen abundance is log ϵ(N) = 8.05 $\pm$ 0.19, which is slightly greater than the solar abundance (marked in this figure by the dotted line).

TABLE 7

UNCERTAINTIES IN THE NLTE ANALYSIS OF NITROGEN

	$\Delta\log\epsilon(N)_{NLTE}$		
	HD 87737	13476	6130
1. ΔT_{eff} = +200 K	+0.05	+0.03	−0.04
2. Δ log g = +0.2	−0.06	−0.02	+0.06
3. $\Delta\ \xi = -1$ km s^{-1}	+0.07	+0.05	+0.08
4. Solar C_{init}	+0.11	+0.12	0.00
5. Photoionization Cross-sections:			
(a) Replace with Hofsaess X-sections	+0.02	+0.02	+0.02
(b) X-sections for Levels *1* to *3* * 0.10	+0.08	+0.01	0.00
6. Line transitions f_{ij} * 0.333	+0.15	+0.09	+0.06
7. Including only 24 line transitions	+0.24	+0.23	+0.10
8. Additional line transitions from OP (total=391)	+0.03	+0.03	+0.03
9. Collisional Ionization Cross-sections:			
(a) X-sections * 10.0	+0.01	0.00	0.00
(b) X-sections * 0.10	0.00	0.00	0.00
(c) Replaced by Drawin formulation	−0.03	−0.01	0.00
10. Collisional Excitation Cross-sections:			
(a) Rad.ly Permitted X-sections * 0.333	−0.08	−0.03	0.00
(b) Rad.ly Forbidden X-sections * 0.10	0.00	0.00	0.00
(c) Rad.ly Forbidden X-sections * 10.0	+0.02	−0.01	+0.01
(d) Replaced Rad.ly Perm. only by Drawin form.	−0.05	−0.02	0.00
(e) Replaced Rad.ly Forb. only by Drawin form.	0.00	−0.01	+0.01
(f) All Replaced by Drawin formulations	−0.05	−0.03	0.00
(g) Drawin formulations * 0.333	−0.12	−0.05	−0.01
11. Collisions with Neutral Particles = 5.0	0.00	0.00	+0.02

"recreate" the LL model since we have included many more atomic levels and have more accurate atomic data, but it shows that it is important to include a sufficiently large number of line transitions in the model for reliable calculations.

5. Increasing the *collision rates with neutral particles* to 5 times the electron excitation rates (as suggested in Tomkin et al. 1992) has no significant effects on the NLTE nitrogen abundances. Changes in the *collisional ionization rates* also had negligible effects on the abundances.

6. The statistical equilibrium of nitrogen in the hotter supergiants is somewhat sensitive to the *electron collisional excitation rates*, as was also found for carbon. If we globally reduce these cross sections by a factor of 3, then the NLTE corrections are increased by $\sim$0.1 dex in the hotter supergiants, but the cooler stars are hardly affected. This is due primarily to the reduction in the collisions between radiatively permitted transitions, which depend on the line strengths; thus uncertainties in the *f*-values are important for these calculations. We also tested replacing the Auer & Mihalas formulae with the Drawin formulae, which caused a marginal increase in the NLTE abundances of the hotter stars, but any perturbations to these cross sections result in similar changes to those found for the Auer & Mihalas formulae rates.

As a test, if we replace these line strength–dependent collision cross sections with an artificially large value, πa_0^2, throughout the model, then the NLTE corrections are decreased by $\sim$0.3 dex in the hotter supergiants, but only $\sim$0.1 dex in the cooler stars. Examining the departure coefficients shows that the occupation numbers of most levels move closer to their LTE values since this test increases the collisional coupling between many levels; thus a trend in N versus $T_{\rm eff}$ remains. Also, the abundances from the quartet and doublet lines are in stark disagreement in this test; the increase in the NLTE abundances are only in the quartet lines (the doublet line abundances do not change significantly). This disagreement strongly suggests that such large collisional coupling is inappropriate in calculating the occupation numbers of nitrogen, but it shows the sensitivity of the nitrogen abundances to the collisional excitation cross sections.

5.3.3. *NLTE Nitrogen Abundance Results for the A-Type Supergiants*

The average NLTE nitrogen abundance that we determine for the 22 A supergiants in this analysis is $\log \epsilon(\mathrm{N/H}) = 8.05 \pm 0.19$, or $\langle[\mathrm{N/H}]\rangle = +0.05 \pm 0.19$. This averaged abundance increases slightly when calculated with respect to iron such that $\langle[\mathrm{N/Fe}]\rangle = +0.16 \pm 0.16$, since $\langle[\mathrm{Fe\ II}]\rangle = -0.11 \pm 0.11$ from all 22 stars. The NLTE nitrogen abundances per star are listed in Table 4. These abundances are in good agreement between several multiplets for all the A-type supergiants examined. In calculating these abundances, we only included the abundances determined from spectral lines with $W_\lambda < 250$ mÅ since other nonclassical effects that are neglected in this analysis (e.g., spherical extension and microvariability) can affect the stronger lines (although we note that the strong lines often yield similar abundances as the weaker lines). The trend seen in the LTE nitrogen abundances is completely removed by these temperature-dependent NLTE abundance corrections, as seen in Figure 9. There are no significant trends seen with gravity (except possibly for the F0 supergiants, which can also be seen in the LTE data). These are the first nitrogen abundances for A-type supergiants calculated using a detailed model atom and careful atmospheric analysis techniques.

Nitrogen line abundance corrections are shown in Table 8 for three representative stars. In the hotter supergiants, the NLTE abundances determined from the doublet line are $\sim$0.1

TABLE 8

NLTE Corrections for Nitrogen Line Abundances

λ	87737			13476			6130		
	W_λ	NLTE	$\Delta\log\epsilon$	W_λ	NLTE	$\Delta\log\epsilon$	W_λ	NLTE	$\Delta\log\epsilon$
$3s^4P - 3p^4S^\circ$:									
7423.62	74	8.07	−0.88	95	7.96	−0.79		...	
7442.28	118	8.08	−1.05	164	7.98	−0.92	92	8.06	−0.41
7468.29	152	8.09	−1.22	214	7.98	−0.93	106	7.98	−0.45
$3s^4P - 3p^4P^\circ$:									
8184.80		...		250	8.05	−1.08	112	7.99	−0.43
8187.95		...		251	8.02	−1.00	150	8.16	−0.49
8210.64		...		128	7.93	−0.70	95	8.05	−0.24
8216.28		...		358	7.88	−1.11	209	7.97	−0.51
8223.07		...		218	7.86	−0.82	130	7.89	−0.31
8242.34		...		216	7.83	−0.81	148	7.98	−0.34
$3s^2P - 3p^2P^\circ$:									
8629.24	167	8.00	−0.85	269	7.74	−1.06	139	7.67	−0.52
$3s^4P - 3p^4D^\circ$:									
8703.24	198	8.14	−1.19	279	8.03	−1.00	144	8.01	−0.38
8711.69	204	8.06	−1.23	306	8.00	−1.06	163	8.02	−0.42
8718.82	178	8.07	−1.11	258	7.99	−0.96		...	
8728.88	74	8.19	−0.77	91	8.07	−0.71		...	

Note.—The values for $\Delta \log \epsilon = \log \epsilon(\mathrm{N})_{\rm NLTE} - \log \epsilon(\mathrm{N})_{\rm LTE}$.

dex larger than those from the quartet lines, which we consider to be very good agreement. When a higher (e.g., solar) carbon abundance is used, then the doublet line abundance was ~0.25 dex larger (with the quartet line abundances unchanged). In the cooler supergiants, the NLTE abundances determined from the doublet line are marginally less than that determined from the quartet lines, e.g., about 0.1–0.2 dex less with the lower carbon abundances. This was an improvement from using a solar carbon abundance, which would raise the quartet line abundances, leaving the doublet correction to be 0.3–0.4 dex less. The remaining differences after using the lower C abundance may not be significant since only one doublet line has been observed in this program (and in only half of the cooler stars), and this line is often moderately strong (~200 mÅ). In future analyses of nitrogen in A supergiants, an effort should be made to observe many N I lines from both the doublet and quartet series.

5.3.4. *Comparisons to Other NLTE Nitrogen Analyses of A–F Supergiants*

Luck & Lambert's (1985) pioneering NLTE analyses of N in F–K supergiants included two F0 supergiants, Canopus and HD 36673. Their same methods and model nitrogen atom were then used by Lambert et al. (1989) to examine the A0 supergiant HD 87737 and by Luck et al. (1990) to examine the high Galactic latitude, A7 supergiant, HD 148743. These analyses found that departures from LTE could enhance the N I lines in the A0–F0 supergiant atmospheres. The NLTE corrections for weak lines were predicted to be near zero, but corrections as large as −1.0 dex were found for the strongest lines. However, these results were based on a very simple N I model atom; for example, they do not include any of the doublet levels or transitions, nor any specific N II levels. Their model includes 13 N I levels plus a continuum level, 15 explicitly calculated bound-bound and bound-free transitions, and an additional nine transitions treated in detailed balance. Compared to our more detailed results, we found that their NLTE nitrogen abundances are too large. Lambert et al. (1989) find the NLTE nitrogen abundance for HD 87737 is log $\epsilon(\mathrm{N})_{\mathrm{NLTE}} \sim 8.4$, whereas we have found ~8.1 dex. The difference is important because 0.3 dex is most of the increase expected if a star has undergone the canonical first dredge-up.

Sadakane, Takeda, & Okyudo (1993) have used Tekeda's (1992) nitrogen model atom and accelerated lambda iteration techniques to estimate the NLTE corrections for the N abundances in two A-type supergiants, Deneb (A2 Ia$^+$) and Rigel (B8 Ia). However, the abundances they determine for these stars are not absolute. First, they have tried to study very luminous supergiants (actually Deneb is a "hypergiant") without considering the limitations of their model atmospheres. Second, they do not determine the atmospheric parameters of these stars; they use average values for temperature based on values in the literature and then adopt a model atmosphere from the Kurucz (1979) grid that has the lowest gravity at that temperature. Third, they have included eight N I lines in their analysis with W_λ's up to 600 mÅ, which is much too strong to use in an abundance analysis even if NLTE is being considered (since uncertainties in the model of the outer atmospheric layers, stellar winds, hydrodynamic effects, and spherical geometry effects are expected to significantly affect strong lines). This analysis by Sadakane et al. only confirms Luck & Lambert's findings that NLTE effects are important for N abundances in A-type supergiants.

6. DISCUSSION

The LTE and NLTE carbon and nitrogen abundances are shown in Figures 6 and 9 and are listed per star in Table 4. We have found that the NLTE corrections are significant for both elements in the atmospheres of the A0–F0 supergiants. For the NLTE carbon abundances, this discussion will only include the results for the A3–F0 supergiants because we consider the NLTE corrections to the C I λ9100 multiplet to be very uncertain, and these lines are the only C I lines observed in the hotter supergiants. Note that we do not discuss the oxygen abundances in the context of CNO cycling, primarily because oxygen is only marginally decreased in comparison to the abundance changes in nitrogen and carbon. The first dredge-up predictions for $\leq 15\ M_\odot$ stars decrease oxygen by ≤0.05 dex (Schaller et al. 1992; Maeder & Meynet 1989; Becker & Iben 1979), and this small change can be easily masked by random uncertainties in an abundance analysis.

6.1. *The Evolutionary Status of A-Type Supergiants Determined from the Carbon and Nitrogen Abundances*

The NLTE nitrogen abundances are roughly solar for all the A-type supergiants we have examined. Since the NLTE carbon abundances are ~0.4 dex less than solar, then the [N/C] ratios are typically 0.4–0.6 dex greater than solar (see Table 4). These ratios are very similar to the first dredge-up predictions for 9–12 $M_\odot$ stars from the Schaller et al. (1992) solar metallicity evolution tracks. Predictions for a 9 $M_\odot$ star after first dredge-up are [N/H] = +0.43, [C/H] = −0.18, and [O/H] = −0.04, yielding [N/C] = 0.6. These predictions are about the same for a 12 $M_\odot$ star, except [N/H] = +0.48. First dredge-up abundances calculated by Becker & Iben (1979) are very similar, even though their models were less sophisticated (e.g., they did not include mass loss or convective overshoot). But, for the A-type supergiants, the [N/C] ratios resemble first dredge-up abundances only because of the low carbon abundances, and not due to any enrichments in nitrogen, *the main feature of the* CNO *cycle*. Furthermore, the lowest luminosity stars have masses of ~5 $M_\odot$, which are *not* expected to be returning from the RGB; see Figure 10 where we plot our program stars on the T_{eff}-gravity plane and include the evolutionary tracks by Schaller et al. (1992).

A better fiducial point than solar abundances would be normal, main-sequence B star abundances, since these are the progenitors for the A-type supergiants. Galactic B star abundances have been determined from detailed model atmosphere analyses by Gies & Lambert (1992), Cunha & Lambert (1994), and Kilian (1992). The B stars are also shown in Figure 10. We would like to calculate a mean carbon and nitrogen abundance for the main-sequence B stars from these surveys.

Each of these B star studies has attempted to account for NLTE effects by using the published NLTE calculations of theoretical equivalent widths for a grid of atmospheric parameters, including temperature, gravity, elemental abundance, and microturbulence (for C II, Eber & Butler 1988; for N II, Becker & Butler 1988b; for O II Becker & Butler 1988a). The NLTE calculations are for line formation only; i.e., line-blanketed, model atmospheres in LTE were adopted from Gold (1984). (Cunha & Lambert note that the Gold model atmospheres are only lightly line blanketed, compared to the most recent atmospheres from Kurucz, which may cause some small differences in the resultant NLTE abundances.) Gies & Lambert have determined LTE and NLTE CNO abundances in 39 B stars selected from the Bright Star Catalogue, which

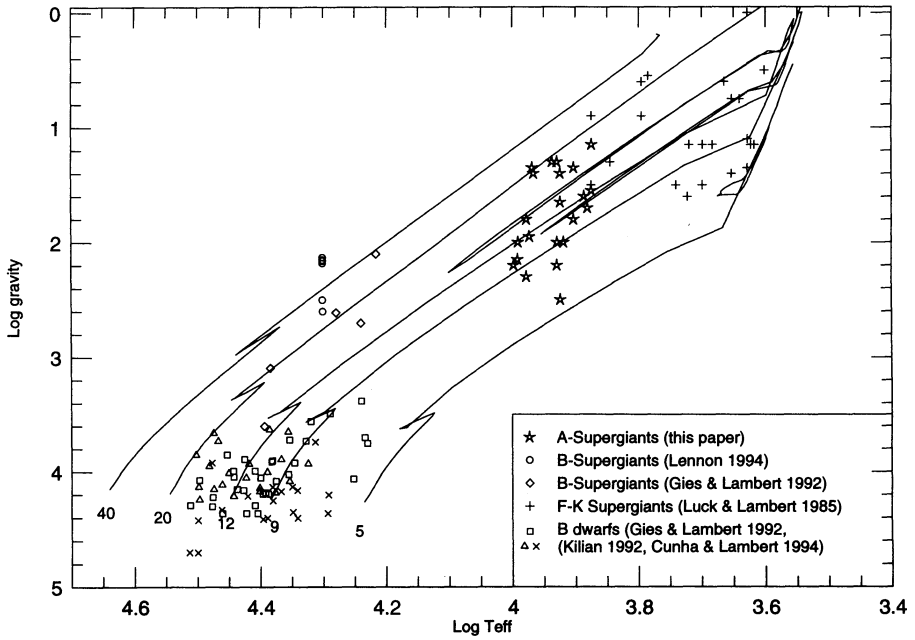

FIG. 10.—Plot of $T_{\rm eff}$ vs. gravity, with stellar evolutionary tracks from Schaller et al. (1992; for 5, 9, 12, 20, and 40 $M_{\odot}$), to show the location of the A-type supergiants analyzed in this paper. Also plotted are the five B supergiants examined by Gies & Lambert (1992) and six B supergiants examined by Lennon (1994). Nonvariable F–K supergiants studied by LL are marked, and the nonsupergiant B stars studied by Gies & Lambert (1992; *unfilled squares*), Cunha & Lambert (1994; *crosses*), and Kilian (1992; *unfilled triangles*).

includes field and cluster stars. Cunha & Lambert have examined the LTE and NLTE CNO abundances in 18 B-type main-sequence stars in the Orion Nebula. Kilian has calculated NLTE CNO abundances in 12 B stars in three clusters and nine field stars. Their mean results for carbon and nitrogen are listed in Table 9, where we have also determined a total mean abundance for all nonsupergiant stars from these analyses (some stars may be counted more than once if analyzed by more than one set of authors). There is very good agreement between these different surveys, with only a few notable exceptions. First, the B-type supergiants examined by Gies & Lambert have significantly different carbon and nitrogen abundances from their nonsupergiant stars, thus only main-sequence B stars are considered for the abundance calculations. Second, Cunha & Lambert have determined marginally higher carbon abundances for Orion OB1 stars than found by Kilian (by about 0.17 dex). Third, Kilian determines a slightly higher nitrogen abundance for field stars than for cluster stars (by 0.21 dex, although the scatter in the field star abundances is quite large, $\sigma = \pm 0.30$ dex) or than the field

TABLE 9

B STAR ABUNDANCES

	C_{NLTE}	C_{LTE}	N_{NLTE}	N_{LTE}
Gies & Lambert (1992) :				
Non-supergiant Stars	8.20 ±0.16 (31)	8.26 ±0.13 (32)	7.81 ±0.12 (34)	7.83 ±0.20 (34)
Field Stars Only	8.27 ±0.12 (6)	8.31 ±0.09 (6)	7.82 ±0.12 (6)	7.79 ±0.11 (6)
Supergiants Only	8.02 ±0.15 (5)	8.21 ±0.14 (5)	8.31 ±0.15 (5)	8.27 ±0.25 (5)
Kilian (1992, 1994) :				
All Stars	8.22 ±0.15 (20)	8.21 ±0.20 (20)	7.78 ±0.27 (21)	7.77 ±0.23 (21)
Field Stars Only	8.24 ±0.23 (8)	8.25 ±0.29 (8)	8.01 ±0.30 (9)	7.91 ±0.24 (9)
Ori OB1 Stars Only	8.25 ±0.05 (7)	8.22 ±0.07 (7)	7.82 ±0.06 (7)	7.70 ±0.06 (7)
Cunha & Lambert (1994) :				
Ori OB1 Stars	8.40 ±0.11 (15)	8.36 ±0.06 (15)	7.76 ±0.13 (15)	7.84 ±0.13 (15)
Mean of Non-Supergiants	8.25 ±0.16 (66)	8.29 ±0.13 (47)	7.79 ±0.22 (70)	7.83 ±0.19 (49)

NOTE.—The mean abundances, $\pm\sigma$, are tabulated. The number of stars used in the mean are shown in parentheses.

stars studied by Gies & Lambert (by 0.09 dex; the mean nitrogen abundance for Gies & Lambert field stars is the same as the mean for all the stars in their survey).

The mean B star abundances that we calculate from these analyses are very similar between the LTE and NLTE abundances, but they are not similar to solar; carbon is less by 0.35 dex and nitrogen by 0.21 dex. Comparing these to the NLTE A supergiant abundances, we find the mean nitrogen abundance of all 22 A-type supergiants is slightly greater than the mean of the B stars; i.e., $\langle \log \epsilon(\mathrm{N/H})_{\mathrm{AI}} - \log \epsilon(\mathrm{N/H})_{\mathrm{B*}} \rangle = +0.26 \pm 0.19$. The mean carbon abundance for the 14 A3–F0 supergiants (where NLTE C could be determined) is very slightly less than the mean value of the B stars; i.e., $\langle \log \epsilon(\mathrm{C/H})_{\mathrm{AI}} - \log \epsilon(\mathrm{C/H})_{\mathrm{B*}} \rangle = -0.11 \pm 0.13$. (The mean NLTE nitrogen abundance for only the 14 A3–F0 supergiants is essentially the same as the mean for all 22 program stars above, $+0.27 \pm 0.21$). The moderately larger N, along with the slightly smaller C indicates that some CN-cycled gas is present at their stellar surfaces.

The mean N/C ratio for the 14 A3–F0 supergiants relative to the B stars is then $\langle \log \epsilon(\mathrm{N/C})_{\mathrm{AI}} - \log \epsilon(\mathrm{N/C})_{\mathrm{B*}} \rangle = +0.38 \pm 0.26$. Individual ratios are listed in Table 4 and plotted relative to T_{eff} in Figure 11; the error bars are from the line-to-line scatter in the NLTE carbon and nitrogen abundances. This mean ratio and most of the individual star ratios are less than the fully mixed, first dredge-up abundance predictions (e.g., by Schaller et al. 1992) that range from [N/C] = +0.65 for 10 $M_{\odot}$ stars to +1.0 for 20 $M_{\odot}$ stars! But, the N/C ratios are also nonzero (with the possible exception of HD 197369 discussed below). Therefore, the N/C ratios relative to the B stars strongly indicate that partial mixing has polluted the stellar surfaces of the A-type supergiants with some CN-cycled products, but the stars have *not* undergone the first dredge-up.

As a consistency check, we have also calculated the sum of the carbon and nitrogen abundances in each star (see Table 4). During the CN cycle, carbon and nitrogen are only used as catalysts for H burning; therefore the relative proportions of these nuclei change, but the sum of the nuclei is conserved. We find $\log \epsilon(\mathrm{C+N})_{\mathrm{AI}} \sim \log \epsilon(\mathrm{C+N})_{\mathrm{B*}}$ to within 0.25 dex throughout, when the abundances relative to iron are used. This is excellent agreement, considering the likely uncertainties in the carbon, nitrogen, and iron abundances.

There are some published evolutionary scenarios that have hypothesized partially mixed CNO abundances in the atmospheres of slightly evolved massive stars. Partial mixing was first proposed by Maeder (1987) for rapidly rotating stars of $\geq 40\ M_{\odot}$ due to internal mixing by turbulent diffusion induced by the rapid rotation. Langer (1992) used this mechanism at LMC metallicities to produce a stellar evolution track for Sk −69°202, progenitor to SN 1987A, so that it would supernova as a blue supergiant. Denissenkov (1994) included turbulent diffusive mixing in 10 $M_{\odot}$ evolution calculations in an attempt to explain the CNO anomalies found by Gies & Lambert (1992) in some evolved B stars.

Complications in comparing A-type supergiant abundances to those from the B stars include the fact that the B stars may experience some mixing with deeper layers while *on* the main sequence. If the main-sequence B stars are already mixed by some unknown amount, our comparison N/C ratio for the B stars would be too high such that the A-type supergiant N/C ratios may be closer to the fully mixed, first dredge-up abundances. The initial B star N/C ratios may not be too far from the initial abundances through, because the mean B star nitrogen abundance is close to the ISM values found recently for the Orion Nebula from optical emission line studies (the average nitrogen abundance for the Orion Nebula is 7.80 ± 0.21 from Baldwin et al. 1991; Rubin et al. 1991; Osterbrock, Tran, & Veilleux 1992; and Peimbert, Storey, & Torres-Peimbert 1993; although optical and IR photoionization analyses often result in wide-ranging nitrogen abundances [Dinerstein 1994; cf. Garnett 1990]). Therefore, the best interpretation available at the moment is to assume that the main-sequence B stars have pristine, cosmic abundances and can be used as the initial abundances for the A supergiants. Thus, the A supergiants have been partially, but not fully, mixed with CN-cycled gas, possibly through internal turbulent mixing induced by rapid rotation near the main sequence. And, therefore, the Population I, A-type supergiants in the Galaxy have evolved directly from the main sequence, contrary to many stellar evolution scenarios, including the popular Schaller et al. (1992) evolution tracks.

The N/C ratios do not depend on the atmospheric temperature, nor on gravity, with the possible exception of the F0 supergiants. Possibly, the low-gravity, i.e., higher luminosity, F0 Ib star HD 36673 has been fully mixed with CN-cycled gas, while one of the high-gravity, i.e., lower luminosity, F0 II stars, HD 196379, may be completely unmixed; see Table 4. These ratios may indicate a gravity/luminosity dependence in the F0 supergiants that is not seen at hotter temperatures (which could be astrophysically interesting), or perhaps these two

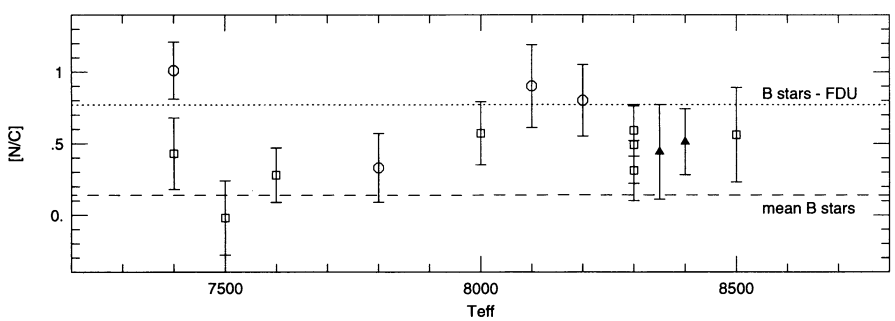

FIG. 11.—NLTE [N/C] ratios are plotted with respect to T_{eff} for the 14 cooler A-type supergiants (where NLTE C could be determined from reliable, weak spectral lines). Error bars represent the line-to-line scatter in the NLTE N and NLTE C abundances. The mean [N/C] ratio of the B stars as calculated here (see text) is shown by the dashed line; the predicted mean [N/C] ratio for the B-stars after the first dredge-up (assuming $M = 10\ M_{\odot}$.) is shown by the dotted line. Notice that the [N/C] ratios of the A-type supergiants tend to be lower than the first dredge-up abundances, but greater than the mean B star ratio, suggestive of partial mixing.

stars are unique; e.g., perhaps their initial CNO abundances were unusual. Gustafsson & Plez (1992) have also found that A–F stars above a certain luminosity may be hydrodynamically unstable; HD 36673 is the only star in our sample that falls within their parameter range, which might have some effects even on the weak line abundances.

6.2. *Comparison to B Supergiant Abundances*

Recent analyses for B-type supergiants by Gies & Lambert (1992) and Lennon (1994) have determined NLTE CNO abundances. The B supergiants that they have examined are shown in Figure 10. The NLTE N/C ratios for the B supergiants relative to the average B star abundances (discussed above) are listed in Table 10. The abundance calculations by Lennon were performed using a grid of theoretical equivalent widths generated from NLTE model atmospheres (including H and He), and using a NLTE line formation code. Similar grids of theoretical equivalent widths (calculated by Becker 1988) were used for Gies & Lambert's NLTE abundances, but only for LTE model atmospheres (Gold 1984) to $\log g = 3.0$. For the supergiant abundances, Gies & Lambert extrapolated this grid to lower gravities and warn that their "NLTE abundances for the supergiants should be treated with caution." Some of the lower luminosity stars from both analyses have NLTE N/C ratios similar to those we have found for the A supergiants; i.e., HD 206165 and 31327 (from Lennon) and HD 52089 (from Gies & Lambert) have $\langle \log \epsilon(\mathrm{N/C})_{\mathrm{BI}} - \log \epsilon(\mathrm{N/C})_{\mathrm{B*}} \rangle = +0.32, +0.43$, and $+0.33$, respectively. Like the A supergiant abundances, these ratios suggest that the B-type supergiants have been *partially* mixed with CN-cycled gas. The star HD 206165 has actually been examined by both authors, yet Gies & Lambert find a larger N/C ratio (that more closely resembles the first dredge-up ratio). Taking their warning, we consider this ratio with caution; first, we notice that the "lower" temperature that they have adopted for this star is ~4000 K less than Lennon's, whereas their "higher" temperature (that they derived from Si II/III/IV ionization equilibrium) is about the same. They have calculated the LTE abundances for both temperatures from Kurucz model atmospheres, and we notice that their LTE and NLTE N/C ratio is similar for the lower temperature. But, their LTE N/C ratio for the higher temperature is only $\langle \log \epsilon(\mathrm{N/C})_{\mathrm{BI}} - \log \epsilon(\mathrm{N/C})_{\mathrm{B*}} \rangle = +0.37$, which is in very good agreement with Lennon's result. The N/C ratio for another low-luminosity B supergiant (HD 51309) studied by Gies & Lambert has a near first dredge-up abundance, but again we find their "high"-temperature LTE abundance is only $\langle \log \epsilon(\mathrm{N/C})_{\mathrm{BI}} - \log \epsilon(\mathrm{N/C})_{\mathrm{B*}} \rangle = +0.38$. Therefore, this B supergiant may also reflect partial mixing of CN-cycled gas in its atmosphere.

The higher luminosity B-type supergiants, with masses between 20 and 25 $M_\odot$ (the B2 Ia and B1 Ib stars), have the largest N/C ratios, ranging from about 1.0 to 2.2 dex greater than the nonsupergiant B stars. These abundances are similar to or greater than the first dredge-up predictions by Schaller et al. (1992; listed in Table 10) for their masses (even though the evolutionary scenarios do not predict that these stars have visited the RGB). This may make these stars distinct from the lower luminosity A- and B-type supergiants. Alternatively, the theoretical NLTE calculations may be less reliable at these higher luminosities, where, for example, a stellar wind component could have significant effects in the line-forming regions of the photosphere.

An interesting sidelight to the analysis of early B-type supergiants are the morphologically distinct BC and BN stars, which are identified by their very weak or very strong nitrogen line strengths, respectively. These subclasses are also found for the nonsupergiant B stars, but the physical processes responsible for the anomalous line strengths may be different for main-sequence and supergiant stars, and other subgroups, e.g., binaries (Walborn 1976). Walborn (cf. 1988) has proposed that the BC supergiants are those stars just leaving the main sequence with pristine compositions, whereas the morphologically "normal" B supergiants and the BN supergiants have undergone partial or full mixing of CN-cycled gas. In support of this, Lennon's (1994) NLTE analysis of a BC2 Ib star has determined that $\langle \log \epsilon(\mathrm{N/C})_{\mathrm{BI}} - \log \epsilon(\mathrm{N/C})_{\mathrm{B*}} \rangle = -0.07$, and Dufton's (1972) LTE analysis of a BC1 Iab supergiant determined that $\langle \log \epsilon(\mathrm{N/C})_{\mathrm{BI}} - \log \epsilon(\mathrm{N/C})_{\mathrm{B*}} \rangle = +0.06$ (we have used their N/C ratios and compared them to the mean B star abundances we calculate above). The abundances are essentially the same as for the normal, unevolved B stars, suggesting no mixing. Also, Smith & Howarth (1994) have analyzed the helium chemistry of an OBC, "normal" OB-type, and OBN supergiant in a detailed NLTE analysis to find that the helium abundance increases between these subtypes, consistent with Walborn's hypothesis. They note that exposing CN-processed material at the surfaces of O supergiants on a necessarily short timescale is an outstanding challenge to evolutionary theory.

TABLE 10

B SUPERGIANT AND FIRST DREDGE-UP ABUNDANCES

	Sp.Ty.	$[\mathrm{N/C}]^{a}_{\mathrm{to\ B*}}$	$[\mathrm{N/C}]^{a}_{\mathrm{to\ B*}}$
B-type Supergiants :			
Gies & Lambert (1992)		NLTE "low" T_{eff}	LTE "high" T_{eff}
HD 91316	B1 Ib	+0.96	+0.95
HD 198478	B3 Ia	+0.98	+0.74
HD 51309	B3 II	+0.78	+0.38
HD 206165[b]	B2 Ib	+0.71	+0.37
HD 52089	B2 II	+0.33	+0.17
Lennon (1994) :		NLTE	
HD 41117	B2 Ia	+2.16	
HD 14818	B2 Ia	+1.46	
HD 14143	B2 Ia	+1.56	
HD 194279	B2 Ia	+1.76	
HD 206165[b]	B2 Ib	+0.32	
HD 31327	B2 II	+0.43	
Theoretical :			
Schaller *et al.* (1992) :		First Dredge-Up	
9 $M_\odot$		+0.63	
12 $M_\odot$		+0.69	
15 $M_\odot$		+0.71	
20 $M_\odot$		+0.98	
25 $M_\odot$		+1.65	

[a] $[\mathrm{N/C}]_{\mathrm{to\ B*}} = \log \epsilon(\mathrm{N/C})_{\mathrm{AI}} - \log \epsilon(\mathrm{N/C})_{\mathrm{B*}}$.
[b] Analyzed by both authors, but with different results; see text.

These stars are slightly more massive than the A supergiants in this paper, but show that OB supergiants do not represent a uniform group in elemental abundances and yet, interestingly, these C and N subclasses do not appear to persist beyond the early B-type supergiants.

6.3. *Comparison to F–K Supergiant Abundances*

We can also compare the carbon and nitrogen abundances for the A-type supergiants to those determined for 25 nonvariable (i.e., not Cepheid variable) F–K supergiants by LL. A few of these stars have been examined by other authors, (e.g., Russell & Bessell 1989; Spite & Spite 1990; Boyarchuk et al. 1985), but their abundances are usually in rough agreement with LL's, and for this discussion we are interested in global properties of yellow supergiants and therefore restrict this discussion to the large data set provided by LL.

Luck & Lambert's program stars are plotted in Figure 10, which shows that most of them have masses similar to the A-type supergiants. We have plotted the N/C ratios for these 25 F–K supergiants relative to the mean B star ratio in Figure 12; the mean value of $\langle \log \epsilon(\mathrm{N/C})_{\mathrm{F-K}} - \log \epsilon(\mathrm{N/C})_{\mathrm{B*}} \rangle = +0.81 \pm 0.34$ (or $[\mathrm{N/C}] = +0.95 \pm 0.34$). This mean value is similar to the first dredge-up predictions (only $\sim$0.2 dex larger), but the scatter is tremendous, with N/C ratios ranging from +0.04 to a remarkable +1.55 relative to the mean B star abundances (see Fig. 12). It is difficult to understand the dispersion in these abundances astrophysically since some of the carbon abundances are depleted by $\sim$0.6 dex and some of the nitrogen abundances are enhanced by $\sim$1.0 dex. Significant mixing of ON-cycled products to drive up the nitrogen abundance is considered by Luck & Lambert (1981, 1985), but regarded as unlikely; the ON cycle requires much higher temperatures to run efficiently, and surface mixing as a red supergiant would have to be much deeper than currently predicted. Also, Luck & Lambert find oxygen abundances for these stars that are roughly equal to those of the normal B stars (i.e., $\sim$0.2 dex less than solar).

Examining the carbon and nitrogen abundances more closely, we notice that the carbon abundances appear to be slightly temperature dependent, which may indicate departures from LTE. Our analysis finds the NLTE corrections for carbon in the F0 supergiants are only $\sim$0.2 dex. A detailed NLTE analysis of the carbon abundances in these stars should be examined. Our NLTE corrections for nitrogen in the F0 supergiants range from 0.2 to 0.4 dex; thus, NLTE effects may be significant for the nitrogen abundances in these yellow supergiants too.

7. CONCLUSIONS

We have calculated LTE and NLTE carbon and nitrogen abundances in a sample of Galactic, A-type supergiants to be used as probes of their evolutionary status. The fundamental results of this paper are as follows:

1. *Departures from LTE must be considered in the line formation calculations when deriving nitrogen and carbon abundances in A supergiants.* NLTE corrections to weak line nitrogen abundances range from −1.0 dex in the A0 supergiants to −0.3 dex in the F0 supergiants. Extensive testing of our new nitrogen model atom shows that the NLTE abundances are not especially sensitive to reasonable uncertainties in the

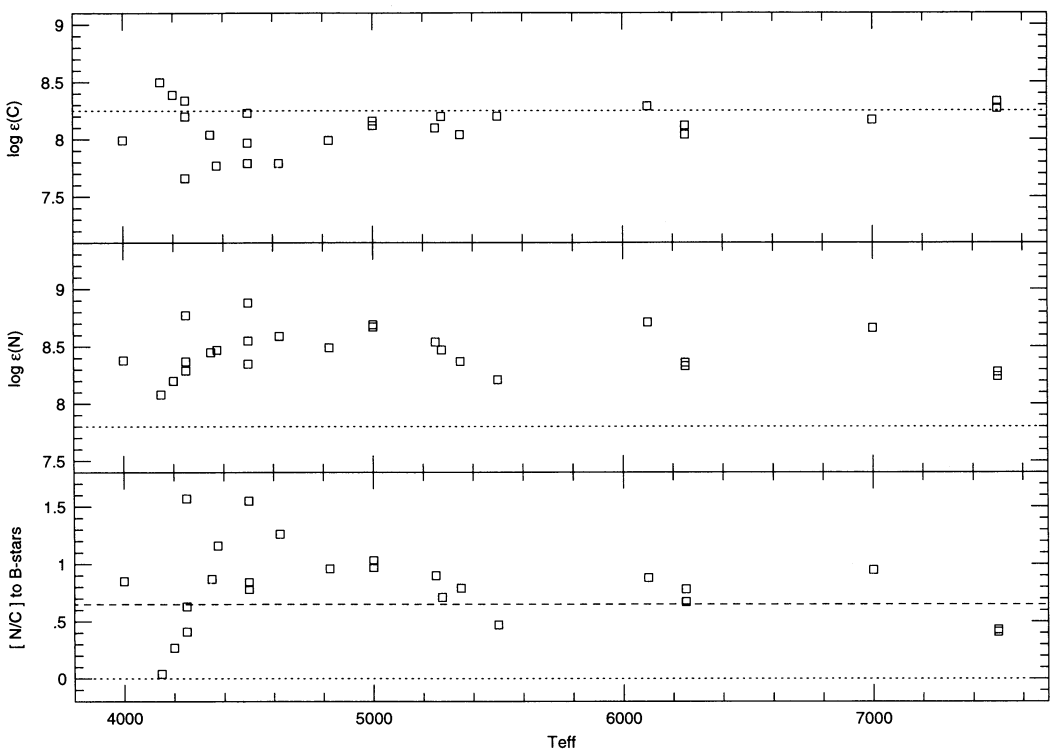

FIG. 12.—LTE carbon and nitrogen abundances found for the F–K supergiants by LL. The nitrogen and carbon abundances have a large scatter, ranging over 1.0 dex each, and resulting in N/C ratios that range over 1.5 dex. Also, the carbon abundances show a temperature dependence that is probably reflective of neglected NLTE effects.

atomic data, with the exception of the electron collisional excitation cross sections and the carbon abundance. The mean NLTE nitrogen abundance for the 22 A0–F0 supergiants in this program is log $\epsilon(N)_{NLTE} = 8.05 \pm 0.19$. The NLTE nitrogen abundances are independent of temperature and gravity, in contrast to the strong dependence on temperature seen in the LTE abundances. Carbon corrections for weak lines range from -0.10 dex in the F0 supergiants to -0.5 dex in the A3 supergiants. We did not calculate NLTE carbon abundances in the A0 supergiants because the C I λ9100 lines that were observed in these stars appear to yield unreliable abundances. The mean NLTE carbon abundance is log $\epsilon(C)_{NLTE} = 8.14 \pm 0.13$ for the 14 A3–F0 supergiants examined. The NLTE carbon abundances also show no dependence on temperature or gravity.

2. *The A supergiants have evolved directly from the main sequence and appear to have undergone partial mixing.* The predicted first dredge-up [N/C] ratio ranges from $+0.65$ for 10 $M_\odot$ stars to $+1.0$ for 20 $M_\odot$ stars, whereas we find the mean N/C ratio of the A supergiants is much less relative to the main-sequence B star abundances, i.e., log $\epsilon(N/C)_{AI} - \log \epsilon(N/C)_{B*} = +0.38 \pm 0.26$. Therefore, these stars appear to have evolved directly from the main sequence and not to have undergone the first dredge-up in a previous red supergiant phase. Since the mean N/C ratio for the A-type supergiants is not the same as for the main-sequence B stars, *partial* mixing of CN-cycled gas is indicated. We suggest this is also indicated in the abundances of *some* evolved B stars.

It is a pleasure to thank Chris Sneden and David Lambert for their help and support throughout this project. Special thanks to Michael Lemke for several tutorials on NLTE, for making his codes available, and for much support. I am grateful to Craig Wheeler, Harriet Dinerstein, John Scalo, and Evan Skillman for their advice and continuous encouragement and to the University of Minnesota for hospitality. This project has benefited greatly from conversations with Doug Gies, Katy Garmany, Ed Fitzpatrick, and Rolf Kudritzki. I am indebted to Danny Lennon, Sylvia Becker, and Norbert Langer for their helpful readings of the manuscript.

REFERENCES

Anders, E., & Grevesse, N. 1989, Geochim. Cosmochim. Acta, 53, 197
Auer, L. H., & Heasley, J. N. 1976, ApJ, 205, 165
Auer, L. H., & Mihalas, D. 1973, ApJ, 184, 151
Baldwin, J. A., Ferland, G. J., Martin, P. G., Corbin M, R., Cota, S. A., Peterson, B. M., & Slettebak, A. 1991, ApJ, 374, 580
Baschek, B., Scholz, M., & Sedlmayr, E. 1977, A&A, 55, 375
Becker, S. A., & Iben, I., Jr. 1979, ApJ, 232, 831
Becker, S. R. 1988, private communication
Becker, S. R., & Butler, K. 1988a, A&AS, 74, 211
———. 1988b, A&AS, 76, 331
Boesgaard, A. M., & Heacox, W. D. 1978, ApJ, 226, 888
Boyarchuk, A. A., Lyubimkov, L. S., & Sakhibullin, N. A. 1985, Astrophysics, 22, 203
Bressan, A., Fagotto, F., Bertelli, G., & Chiosi, C. 1993, A&AS, 100, 647
Chiosi, C., Nasi, E., & Sreenivasan, S. R. 1978, A&A, 63, 103
Chiosi, C., & Summa, C. 1970, Ap&SS, 8, 478
Cunha, K., & Lambert, D. L. 1994, ApJ, 426, 170
Denissenkov, P. A. 1994, A&A, 287, 113
Dinerstein, H. L. 1994, private communication
Drawin, H. W. 1967, Collision and Transport Cross-Sections, (Rep. EUR-CEA-FC-383) (Fontenay-aux-Roses: Assoc. Euratom-CEA)
Dufton, P. L. 1972, A&A, 16, 301
Eber, F., & Butler, K. 1988, A&A, 202, 153
El Eid, M. F. 1994, A&A, 285, 915
Fitzpatrick, E. L., & Garmany, C. D. 1990, ApJ, 363, 119
Garnett, D. R. 1990, ApJ, 363, 142
Gies, D. R., & Lambert, D. L. 1992, ApJ, 387, 673
Gold, M. 1984, Ph.D. thesis, Diplomarbeit Univ. München
Grevesse, N., Lambert, D. L., Sauval, A. J., van Dishoeck, E. F., Farmer, C. B., & Norton, R. H. 1990, A&A, 232, 225
———. 1991, A&A, 242, 488
Gustafsson, B., & Plez., B. 1992, in Instabilities in Evolved Super- and Hypergiants, ed. C. de Jager & H. Nieuwenhuijzen (Amsterdam: North-Holland), 86
Hibbert, A., Biémont, E., Godefroid, M., & Vaeck, N. 1991a, A&AS, 88, 505
———. 1991b, J. Phys B, 24, 3943
———. 1993, A&AS, 99, 177
Hofsaess, D. 1979, Atomic Data Nucl. Data Tables, 24, 285
Iben, I., Jr. 1966, ApJ, 143, 516
Ivanova, Z. K., & Lyubimkov, L. S. 1990, Bull. Crimean Astrophys. Obs., 79, 45
Kilian, J. 1992, A&A, 262, 171
Kudritzki, R. P. 1992, A&A, 266, 395
Kurucz, R. L. 1979, ApJS, 40, 1
———. 1991, private communication
Lambert, D. L., Hinkle, K. H., & Luck, R. E. 1989, ApJ, 333, 917
Lambert, D. L., Roby, S. W., & Bell, R. A. 1982, ApJ, 254, 663
Langer, N. 1992, A&A, 265, L17
———. 1994, private communication
Langer, N., & Maeder, A. 1995, A&A, 295, 685
Lemke, M., & Venn, K. A. 1995, in preparation
Lennon, D. J. 1994, Space Sci. Rev., 66, 127
Luck, R. E., Bond, H. E., & Lambert, D. L. 1990, ApJ, 357, 188
———. 1985, ApJ, 298, 782 (LL)
Luck, R. E., & Lambert, D. L. 1981, ApJ, 245, 1018
Maeder, A. 1987, A&A, 178, 159
Maeder, A., & Meynet, G. 1989, A&A, 210, 155
Mihalas, D. 1978, Stellar Atmospheres (2d ed.; San Francisco: Freeman)
Moore, C. E. 1970, NSRDS-NBS 3, § 3
———. 1975, NSRDS-NBS 3, § 5
———. 1976, NSRDS-NBS 3, § 7
Nussbaumer, H., & Storey, P. J. 1984, A&A, 140, 383
Osterbrock, D. E., Tran, H. D., & Veilleux, S. 1992, ApJ, 389, 305
Peimbert, M., Storey, P. J., & Torres-Peimbert, S. 1993, ApJ, 414, 626
Rubin, R. H., Simpson, J. P., Haas, M. R., & Erickson, E. F. 1991, ApJ, 374, 564
Russell, S. C., & Bessell, M. S. 1989, ApJS, 70, 865
Sadakane, K., Takeda, Y., & Okyudo, M. 1993, PASJ, 45, 471
Schaller, G., Schaerer, D., Meynet, G., & Maeder, A. 1992, A&AS, 96, 269
Smith, K. C., & Howarth, I. D. 1994, A&A, 290, 868
Spite, M., & Spite, F. 1990, A&A, 234, 67
Stothers, R. B., & Chin, C. 1973, ApJ, 179, 555
———. 1976, ApJ, 204, 472
———. 1991, ApJ, 381, L67
Stürenberg, S., & Holweger, H. 1990, A&A, 237, 125 (SH)
Takeda, Y. 1992, PASJ, 44, 649
Tomkin, J., & Lambert, D. L. 1994, PASP, 106, 365
Tomkin, J., Lemke, M., Lambert, D. L., & Sneden, C. 1992, AJ, 104, 1568
van Regemorter, H. 1962, ApJ, 136, 906
Venn, K. A. 1993, ApJ, 414, 316
———. 1995, ApJS, 99, 659
Walborn, N. R. 1976, ApJ, 205, 419
———. 1988, in IAU Collog. 108, Atmospheric Diagnostics of Stellar Evolution, ed. K. Nomoto (Berlin: Springer), 70
Zhu, Q., Bridges, J. M., Hahn, T., & Wiese, W. L. 1989, Phys. Rev. A, 40, 3721